

**TECHNICAL REPORT  
NATICK/TR-15/008**



**AD \_\_\_\_\_**

# **ULTRASONIC COATING AND HOLOGRAPHIC EXPOSURE TECHNOLOGY PHASE I**

**by  
Matt Kinzler  
and  
Shaun Abraham**

**Revision Military Technologies  
Essex Junction, VT 05452**

**September 2015**

**Final Report  
June 2013 – May 2014**

**Approved for public release; distribution is unlimited**

**Prepared for  
U.S. Army Natick Soldier Research, Development and Engineering Center  
Natick, Massachusetts 01760-5020**

## DISCLAIMERS

The findings contained in this report are not to be construed as an official Department of the Army position unless so designated by other authorized documents.

Citation of trade names in this report does not constitute an official endorsement or approval of the use of such items.

## DESTRUCTION NOTICE

### For Classified Documents:

Follow the procedures in DoD 5200.22-M, Industrial Security Manual, Section II-19 or DoD 5200.1-R, Information Security Program Regulation, Chapter IX.

### For Unclassified/Limited Distribution Documents:

Destroy by any method that prevents disclosure of contents or reconstruction of the document.

REPORT DOCUMENTATION PAGE					Form Approved OMB No. 0704-0188	
Public reporting burden for this collection of information is estimated to average 1 hour per response, including the time for reviewing instructions, searching existing data sources, gathering and maintaining the data needed, and completing and reviewing this collection of information. Send comments regarding this burden estimate or any other aspect of this collection of information, including suggestions for reducing this burden to Department of Defense, Washington Headquarters Services, Directorate for Information Operations and Reports (0704-0188), 1215 Jefferson Davis Highway, Suite 1204, Arlington, VA 22202-4302. Respondents should be aware that notwithstanding any other provision of law, no person shall be subject to any penalty for failing to comply with a collection of information if it does not display a currently valid OMB control number.						
PLEASE DO NOT RETURN YOUR FORM TO THE ABOVE ADDRESS.						
1. REPORT DATE (DD-MM-YYYY) 10-09-2015		2. REPORT TYPE Final		3. DATES COVERED (From - To) June 2013 – May 2014		
4. TITLE AND SUBTITLE  ULTRASONIC COATING AND HOLOGRAPHIC EXPOSURE TECHNOLOGY - PHASE I				5a. CONTRACT NUMBER W911QY-13-C-0080		
				5b. GRANT NUMBER		
				5c. PROGRAM ELEMENT NUMBER		
6. AUTHOR(S)  Matt Kinzler and Shaun Abraham				5d. PROJECT NUMBER		
				5e. TASK NUMBER		
				5f. WORK UNIT NUMBER		
7. PERFORMING ORGANIZATION NAME(S) AND ADDRESS(ES) Revision Military Technologies 36 River Road Essex Junction, VT 05452				8. PERFORMING ORGANIZATION REPORT NUMBER		
9. SPONSORING / MONITORING AGENCY NAME(S) AND ADDRESS(ES) U.S. Army Natick Soldier Research, Development and Engineering Center General Greene Avenue, ATTN: RDNS-WSB-N (P. Stenhouse) Natick, MA 01760-5020				10. SPONSOR/MONITOR'S ACRONYM(S) NSRDEC		
				11. SPONSOR/MONITOR'S REPORT NUMBER(S) NATICK/TR-15/008		
12. DISTRIBUTION / AVAILABILITY STATEMENT Approved for public release; distribution is unlimited.						
13. SUPPLEMENTARY NOTES						
14. ABSTRACT This report describes research efforts by Revision Military Technologies, LLC. in the development of an ultrasonic coating and holographic exposure technology to apply diffraction gratings onto planar substrates. An ultrasonic coater is used to apply a thin film of a photosensitive azobenzene layer to a hard coated polycarbonate substrate, which is then irradiated with a 442 nm wavelength laser to expose a diffraction grating pattern. Then, the substrate is over-coated with a liquid crystal monomer to develop the diffraction grating. Crystallization and dewetting indicated a chemical incompatibility between the azobenzene and liquid crystal, and improvements in chemistry were suggested in advance of Phase II.						
15. SUBJECT TERMS  ALIGNMENT                      HOLOGRAPHY                      LIQUID CRYSTALS SUBSTRATES                    AZOBENZENES                   POLYCARBONATES DIFFRACTION                   ULTRASONICS                    PHOTSENSITIVITY LASER BEAMS     GRATINGS(SPECTRA)						
16. SECURITY CLASSIFICATION OF:			17. LIMITATION OF ABSTRACT	18. NUMBER OF PAGES	19a. NAME OF RESPONSIBLE PERSON	
a. REPORT	b. ABSTRACT	c. THIS PAGE			Peter Stenhouse	
U	U	U	SAR	52	19b. TELEPHONE NUMBER (include area code) 508-233-6166	

This page intentionally left blank

## TABLE OF CONTENTS

Section	Page
<b>LIST OF FIGURES .....</b>	<b>iv</b>
<b>LIST OF TABLES .....</b>	<b>vii</b>
<b>1.0 INTRODUCTION .....</b>	<b>1</b>
<b>2.0 METHODS, ASSUMPTIONS, AND PROCEDURES .....</b>	<b>2</b>
<b>2.1 Schedule and Budget Performance .....</b>	<b>2</b>
<b>2.2 Kickoff Meeting .....</b>	<b>4</b>
<b>2.3 Technical Accomplishments .....</b>	<b>4</b>
2.3.1 <i>Coating System .....</i>	<i>4</i>
2.3.1.1 AZB Deposition .....	5
2.3.1.2 Corona Discharge Effect on Ballistics .....	8
2.3.1.3 AZB Thin Film Process Improvements .....	9
2.3.1.4 LC Deposition .....	11
2.3.1.5 Crystallization Defects and Local Dewetting at Room Temperature .....	13
2.3.1.6 High and Low Temperature Tests .....	15
2.3.1.7 Mixed Solvents .....	17
2.3.1.8 Spray Coating with Lower Boiling Point Solvents .....	18
2.3.1.9 Spray Coating with Elevated Substrate Temperature .....	20
2.3.1.10 Onsite Testing at USI .....	24
2.3.1.11 Theoretical Model for the LC Film .....	27
2.3.2 <i>Irradiation System .....</i>	<i>27</i>
2.3.3 <i>Curing System .....</i>	<i>29</i>
2.3.4 <i>Plaque Tooling and Production .....</i>	<i>30</i>
2.3.5 <i>Imaging Metrology .....</i>	<i>30</i>
2.3.6 <i>Root Cause Analysis of Dewetting at AZB and LC Layer Interface .....</i>	<i>31</i>
<b>3.0 RESULTS AND DISCUSSION .....</b>	<b>35</b>
<b>4.0 CONCLUSIONS .....</b>	<b>38</b>
<b>4.1 Implications for Future Work .....</b>	<b>39</b>
<b>5.0 REFERENCES .....</b>	<b>40</b>
<b>List of Symbols, Abbreviations, and Acronyms .....</b>	<b>41</b>

## LIST OF FIGURES

Figure	Page
Figure 1 - Schedule .....	3
Figure 2 - Spray Coater .....	4
Figure 3 - Flame treatment, glass, 10x .....	7
Figure 4 - Bleach soak, glass, 10x .....	7
Figure 5 - Corona discharge, glass, 10x .....	7
Figure 6 - Flame treatment, glass, 56x .....	7
Figure 7 - Bleach soak, glass, 56x .....	7
Figure 8 - Corona discharge, glass, 56x .....	7
Figure 9 - No wash, hardcoated polycarbonate, 10x .....	8
Figure 10 - Corona discharge, HCPC, two sweeps, 10x .....	8
Figure 11 - Corona discharge, HCPC, six sweeps, 10x .....	8
Figure 12 - No wash, HCPC, 56x .....	8
Figure 13 - Corona discharge, HCPC, two sweeps, 56x .....	8
Figure 14 - Corona discharge, HCPC, six sweeps, 56x .....	8
Figure 15 - No corona .....	9
Figure 16 - Six pass corona .....	9
Figure 17 - 45 s corona .....	9
Figure 18 - No corona, zoom view .....	9
Figure 19 - Six pass corona, zoom view .....	9
Figure 20 - 45 s corona, zoom view .....	9
Figure 21 - AZB poor coating with rough surface .....	10
Figure 22 - AZB with smoother surface .....	10
Figure 23 - AZB with smoothest surface .....	10
Figure 24 - AZB/Grating/LC on polycarbonate under differential interference contrast (DIC) illumination .....	10
Figure 25 - AZB/Grating/LC on polycarbonate under DIC .....	10
Figure 26 - Local Dewetting on polycarbonate with grating visible .....	10
Figure 27 - LC on AZB .....	14
Figure 28 - LC on AZB, wavy .....	14
Figure 29 - LC on AZB, local dewetting .....	14
Figure 30 - Solid crystal nucleation sites .....	14
Figure 31 - Crystal, high magnification .....	14
Figure 32 - Reference blank .....	14
Figure 33 - Thick LC film with crystallization .....	14
Figure 34 - Crystallization, polarized light .....	14
Figure 35 - Crystallization with boundaries .....	14
Figure 36 - Feather-like crystals .....	14
Figure 37 - Spherulitic structure, polarized light .....	14
Figure 38 - Crystals, boundaries, and local dewetting region .....	14
Figure 39 - Panoramic view of crystal growth .....	15
Figure 40 - Spherulitic structure, low temp .....	15
Figure 41 - Feather-like structures, low temp .....	15
Figure 42 - Radial crystal growth, low temp .....	15
Figure 43 - Feather-like structures, high-range focus .....	15
Figure 44 - Feather-like structure, mid-range focus .....	15
Figure 45 - Feather-like structure, low-range focus .....	15
Figure 46 - Local dewetting .....	16

Figure 47 - Local dewetting, zoom .....	16
Figure 48 - Water condensation on AZB/LC.....	16
Figure 49 - Local dewetting, wavy surface after exposure to condensed water .....	16
Figure 50 - Dewetting, low magnification .....	16
Figure 51 - Dewetting, high magnification .....	16
Figure 52 - High temp dewetting, 'lakes' .....	17
Figure 53 - High temp dewetting, 'islands'.....	17
Figure 54 - High temp dewetting, crystallization boundary .....	17
Figure 55 - LC solvent exchange facilitated by evaporation with nitrogen stream .....	19
Figure 56 - LC in MEK, spin coated onto AZB spin coated glass; with diffraction grating. ....	20
Figure 57 - Local dewetting of LC in MEK, spray coated onto spin coated AZB spin coated HCPC. ....	20
Figure 58 - Crystallization of spin coated LC in MEK over a period of 24 hours.....	20
Figure 59 - LC spray coated onto spin coated AZB glass, center area. ....	21
Figure 60 - LC spray coated onto spin coated AZB glass, boundary area. ....	21
Figure 61 - Macroscopic view of spray coat pattern on glass. Transparent area was irradiated. Boundary area observable.....	21
Figure 62 - LC spray coated onto spin coated AZB HCPC, center area.....	22
Figure 63 - LC spray coated onto spin coated AZB HCPC, boundary area local dewetting. ....	22
Figure 64 - Macroscopic view of LC spray coat pattern on HCPC. Boundary area observable. Pooling of coating observable at start position. ....	22
Figure 65 - Parallel line LC spray coating. Boundary of spray pattern visible.....	22
Figure 66 - Serpentine LC spray coating. Boundary not visible. Obvious disruption of film. ....	22
Figure 67 - LC spray coated onto AZB spray coated HCPC, center region. ....	23
Figure 68 - LC spray coated onto AZB spray coated HCPC, boundary region. ....	23
Figure 69 - Macroscopic view of LC spray coating.....	23
Figure 70 - AZB spray coated onto HCPC. ....	23
Figure 71 - Local dewetting of spray coated LC on spray coated AZB HCPC. ....	23
Figure 72 - Spray coated LC on spray coated AZB. ....	23
Figure 73 - Central and Boundary regions of spray coated LC .....	24
Figure 74 - Mylar coated with LC .....	26
Figure 75 - Glass AZB substrate coated with LC, typical dewetting.....	26
Figure 76 - Glass AZB substrate coated with LC, strong tendency for dewetting .....	26
Figure 77 - Glass and PC AZB substrates with LC; different degrees of dewetting .....	26
Figure 78 - UCHET on glass, new exposure system, 0° rotation .....	28
Figure 79 - UCHET on glass, new exposure system, 90° rotation .....	28
Figure 80 - UCHET on polycarbonate, new exposure system.....	28
Figure 81 - Optical Alignment and Collimation .....	29
Figure 82 - Optical fixturing system. ....	29
Figure 83 - Fixturing system on an alignment rail. ....	29
Figure 84 - Curing Oven .....	30
Figure 85 - Uniform alignment layer .....	31
Figure 86 - Blank substrate .....	31
Figure 87 - Topographic Map .....	31
Figure 88 - Thickness distribution (nm) .....	31
Figure 89 - Highly polarized surfactant molecules demonstrating hydrophobic and hydrophilic conditions (J. Ruchmann, 2008).....	32
Figure 90 - Cis-trans conformation change(J. Ruchmann, 2008) .....	33
Figure 91 - Surface profile of the AZB coating on hard-coated PC plaque.....	35
Figure 92 - Reference dye coating, reflected light.....	35
Figure 93 - Partial crystallization.....	36
Figure 94 - LC coated and patterned PC samples after 5 days, cross polarizers .....	37

Figure 95 - LC coated and patterned PC samples after 1 month storage, cross polarizers .....	37
Figure 96 - Comparison of samples just produced and the one stored for ~ 2 months, observed in reflected light on black background.....	37



## LIST OF TABLES

Table	Page
Table 1 - AZB test matrix .....	6
Table 2 - LC test matrix .....	12
Table 3 - Experimental design for LC spray coat test, with temperature as dependent variable. ....	21
Table 4 - USI LC spray coating conditions and results .....	26

This page intentionally left blank

# ULTRASONIC COATING AND HOLOGRAPHIC EXPOSURE TECHNOLOGY PHASE I

## 1.0 INTRODUCTION

The Ultrasonic Coating and Holographic Exposure Technology (UCHET) program was initiated by Revision Military Technologies in August 2013 to explore novel methods to deposit and functionalize optical thin films onto planar and spherical lenses. The U.S. Army is interested in depositing these advanced coatings onto the same substrates used for soldier ballistic eye protection. The coating techniques will enable new protection modalities for soldiers against high intensity laser radiation threats. This report details our Phase I laboratory based research, development and demonstration efforts that were completed through a contract with the Natick Soldier Research, Development and Engineering Center (NSRDEC) from June 2013 to May 2014. The ultimate goal of this work is to develop procedures that produce effective eye protection that can be implemented in a high-volume manufacturing environment.

In this phase, we (1) developed a multi-unit die tool for producing planar plaques of consistent quality in large quantities, (2) developed a surface treatment process to enhance the wetting of azobenzene (AZB) onto hardcoated polycarbonate (HCPC) plaques, (3) developed the optimized processing parameters for the deposition of AZB via spray coating, (4) developed the processing parameters for the deposition of liquid crystal (LC) via spray coating onto AZB coated plaques, (5) performed significant analysis into the observed LC incompatibility with the AZB layer, (6) developed a surface analysis technique for studying roughness and defects, (7) developed an exposure system for the irradiation of AZB coated plaques, and (8) developed a curing system to crosslink the LC monomers.

UCHET is a combination of two techniques that allow for the deposition of thin films using an ultrasonic spray coater and patterning of the films using an ultraviolet (UV) laser. The main objectives for this project are the development of technology for deposition of thin films on a plaque or lens, functionalization of these films using ultraviolet irradiation with a master grating, and curing of the films. The layers include a photosensitive AZB moiety and a polymer LC. The AZB layer is irradiated with a 110 mW helium-cadmium laser (442 nm,  $\sim 15 \text{ mW/cm}^2$  at the substrate) which passes through a master grating. The master grating orients the laser beam writing a unique polarization pattern in the AZB film. Subsequently an LC monomer is applied over the AZB layer where the LC crystallizes under the direction of the underlying AZB polarization pattern.

Phase 1 of the UCHET program involved the development of technology to deposit and irradiate thin film, siloxane HCPC planar plaques. Specific Phase 1 goals included: develop a method to produce plaques in quantity, establish a *Process of Record* to prepare the substrates, determine proper ultrasonic spray coating parameters and material preparation requirements for ultra-thin films of AZB and LC, construct an exposure station for efficient irradiation of AZB, develop a curing system, and summarize the above findings in a final report with associated deliverables.

## **2.0 METHODS, ASSUMPTIONS, AND PROCEDURES**

Materials for the UCHET program include an AZB photoalignment moiety and a polymer LC, both supplied by Beam Engineering for Advanced Measurements, Inc. located in Winter Park, Florida. Beam also supplied the master polarization gratings for patterning the AZB layer. A Prism 300 spray coater was previously purchased from Ultrasonic Systems, Inc. located in Haverhill, Massachusetts. A helium-cadmium, dual wavelength laser was previously purchased from Kimmon-Koha in Fukushima, Japan. The spray coater and laser constitute the bulk of the essential equipment required to execute this effort. Other laboratory equipment and tools were also required, and include such items as a corona discharge device, a UV curing oven, hot plate, and jigging for optics that were fabricated at Revision.

Test plaques for process development and evaluation were molded at Revision and flow coated with standard hard coat on the coating line in Essex Junction, VT. Plaques were washed and sonicated in isopropanol, and dried with nitrogen prior to use.

### **2.1 Schedule and Budget Performance**

The program was successfully executed according to the outlined schedule in the Statement of Work given in Figure 1. A two month no-cost extension was approved by Landa Hoke on 3/12/2014. Technical and experimentation objectives were completed by the end of the period of performance date of April 30, 2013 with data validation and re-testing continuing through the final report for quality purposes. Expenditures charged to this program were within budget. The subcontracts with Advanced Photon Sciences, LLC were completed within budget.

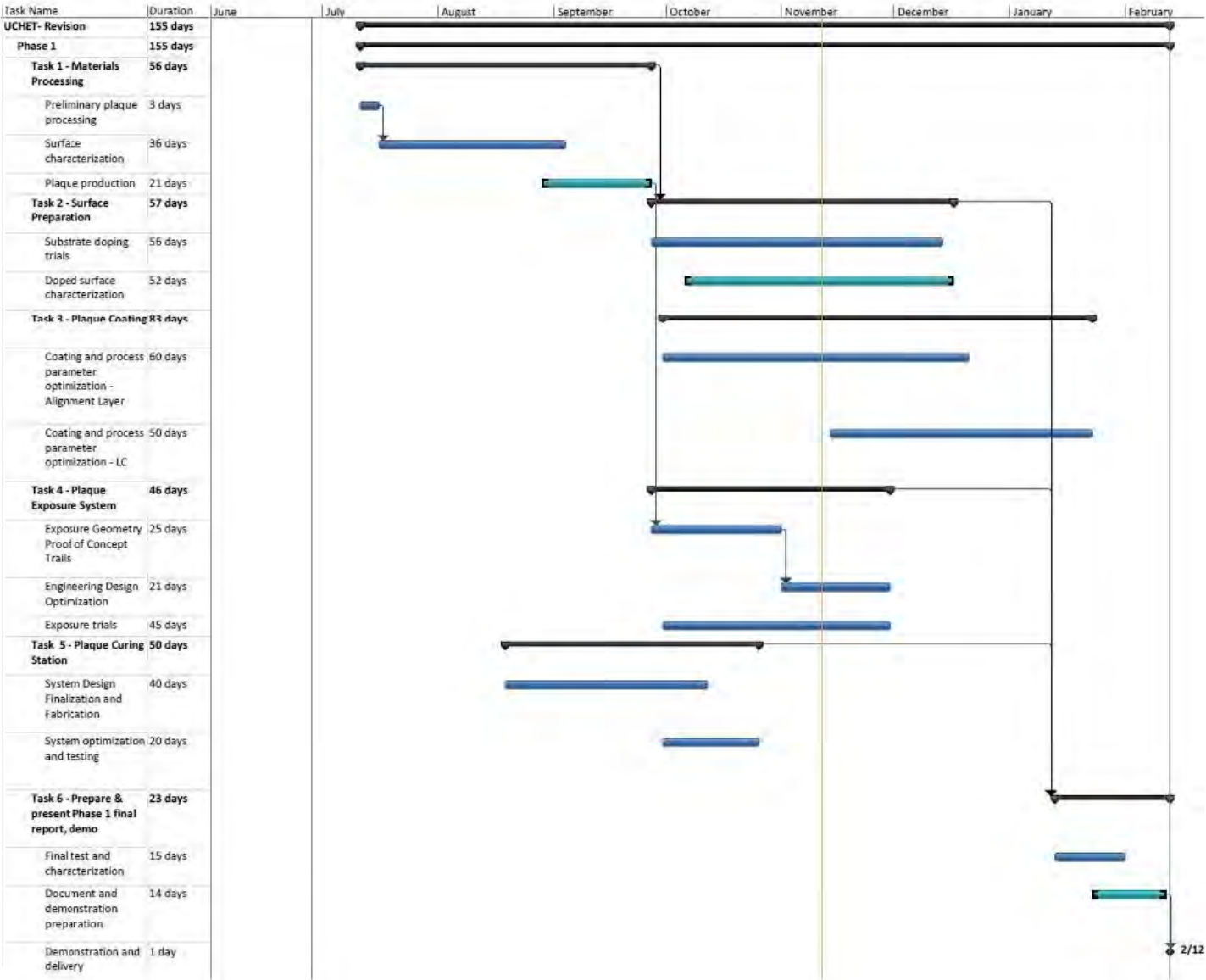


Figure 1 - Schedule

## 2.2 Kickoff Meeting

A kick off meeting was held via teleconference on July 24, 2012. In attendance were Dr. Brian Kimball, Michelle Markey, Landa Hoke, and Stephen Abate of NSRDEC and Dave Puckett, Shaun Abraham, Matt Kinzler, Oliver Pentenrieder, and Garth Blocher of Revision Military Technologies.

## 2.3 Technical Accomplishments

### 2.3.1 Coating System

Revision used a USI Prism 300 ultrasonic spray coater for UCHET Phase 1 (Figure 2). The spray coater has a robotic gantry with x, y, z, and  $\theta$  motion capability. The spray coating liquid is fed to the nozzle via a syringe pump which can supply liquid at a rate of 0.31 mL/min to 10 mL/min. Atomization occurs with an ultrasonic transducer that vibrates at 45 kHz. The plume of atomized liquid is delivered to the substrate via nitrogen airflow, which can be adjusted continuously from 0 to 60 psi. The coating conditions that can be programmed include: pattern, mass flow rate, pressure, height, gantry speed, ultrasonic frequency (seven settings), and  $\theta$  ( $0^\circ$  or  $90^\circ$  with respect to x). In addition, a hot plate was installed in the spray coating chamber, which can be used to heat substrates from 25 °C to 150 °C.



Figure 2 - Spray Coater

To improve wettability of samples by AZB solution, the samples were exposed to corona discharge. The plaques were placed on an insulating stage and exposed to the filament corona discharge for six to ten sweeps. The spray coater was purged with methanol, the solvent for the AZB, and then AZB in methanol was loaded into the syringe. The plaques were placed into the chamber of the spray coater and coated with a thin film of AZB. The plaques were removed from

the spray coater and placed in the optics mount in line with the laser and the master grating. The plaque was exposed to laser radiation for a predetermined period of time. The irradiated plaques were stored in a dry box with continuous nitrogen flow while the spray coater was purged with methanol and cyclopentanone. LC solution in cyclopentanone was loaded into the spray coater syringe and the subsequent plaques were placed onto the heating plate in the spray chamber. The plaques were coated with LC at selected conditions, and after drying they were cured with UV light in the system purged with nitrogen.

#### 2.3.1.1 AZB Deposition

AZB (claimed to be ~1% in methanol and other solvents) was loaded into the spray coater with a dilution of 1:10 in methanol. The coating conditions used were: flow rate = 1.0 mL/min, pressure = 60 psi, height = 120 mm, gantry speed = 100 mm/s, temperature = 50 °C, ultrasonic power = one above lowest setting. The spray coater sprays a serpentine pattern over the selected plaque area (2 cm x 3 cm).

The initial wetting of the AZB monomer on glass and polycarbonate was poor, and there was a strong tendency for physical dewetting of the liquid droplets upon contact with the substrate surface. This is a common phenomenon in coating science, and the steps to mitigate dewetting typically include a surface treatment process prior to coating designed to improve the attraction between the molecules of the coating and the surface molecules on the substrate.

A test matrix was designed to optimize coating conditions for the AZB layer. We ranked the process parameters in order of what we thought had the most effect to the least effect on the coating, as shown in Table 1.

Our initial hypothesis was based primarily on the previous work, in which we coated the alignment layer onto HCPC plaques and consistently observed spotting and clumping of the coating rather than formation of a uniform film. It suggested that surface wetting was the primary factor that needed to be improved. Temperature, flow rate, and distance between the spray-head and the substrate were chosen as the most important contributors to forming the uniform film. The rationale behind it is related to the dynamic character of the film deposition. Behavior of the microdroplets impacting the substrate, their coalescence, solvent evaporation and final film forming or dewetting depend on surface tension, viscosity, and local temperature, which all rapidly change during the process.

Table 1 - AZB test matrix

Parameters	Levels	Parameters	Levels
<b>Temp:</b> Substrate temperature [°C]	25/40/60	<b>Dist:</b> Nozzle-substrate distance [mm]	40/80/120
<b>Velocity:</b> Nozzle scan rate [mm/s]	10/40/100	<b>Pres:</b> Nitrogen pressure [psi]	20/40/60
<b>Flow:</b> Solution flow rate [mL/min]	0.31/0.45/0.62	<b>Pass:</b> number of passes	1/2/3

Temp	Flow	Dist	Pres	Velocity	Pass
25	0.31	40	20	10/40/100	1,2,3
			40	10/40/100	1,2,3
			60	10/40/100	1,2,3
		80	20	10/40/100	1,2,3
			40	10/40/100	1,2,3
			60	10/40/100	1,2,3
		120	20	10/40/100	1,2,3
			40	10/40/100	1,2,3
			60	10/40/100	1,2,3
	0.45	40	20	10/40/100	1,2,3
			40	10/40/100	1,2,3
			60	10/40/100	1,2,3
		80	20	10/40/100	1,2,3
			40	10/40/100	1,2,3
			60	10/40/100	1,2,3
		120	20	10/40/100	1,2,3
			40	10/40/100	1,2,3
			60	10/40/100	1,2,3
	0.62	40	20	10/40/100	1,2,3
			40	10/40/100	1,2,3
			60	10/40/100	1,2,3
		80	20	10/40/100	1,2,3
			40	10/40/100	1,2,3
			60	10/40/100	1,2,3
		120	20	10/40/100	1,2,3
			40	10/40/100	1,2,3
			60	10/40/100	1,2,3

The substrates we used in our experiments were: glass 1 x 1 inch and HCPC plaques 2 x 2 inches. The coating solutions were claimed to be: 0.36% by weight in methanol; 1% by weight in dimethyl formamide (DMF) though we suspect concentrations to be as high as 10%. For the case of no treatment on glass, we sonicated substrate and washed with deionized (DI) water and dried with N<sub>2</sub>. For the cleaning treatment case on glass, we sonicated the substrate in soap, methanol, acetone or toluene and dried with N<sub>2</sub>. For the chemical treatment case on glass, we soaked the substrate in sodium hypochlorite (bleach) for 1 min or sulphuric acid for 30 s, rinsed with DI water, and dried with N<sub>2</sub>. For the case of surface treatment on glass, we sonicated and washed substrates with DI water; dried with N<sub>2</sub>; and then exposed the surface to corona or flame treatment.



We recognized that spray coating physics should be similar for glass and polycarbonate, particularly the behavior of spray droplets from the nozzle to the time right before coating hits substrate. However, we understood that the interaction of spray droplets with substrate would likely be different between glass and HCPC. This is thought to be due to differences in surface energy and surface roughness; plus, the effects of cleaning and surface treatment would likely yield different results on different materials.

After unsuccessfully coating a uniform thin film without surface treatment on glass, the various treatment methods were applied to the glass substrate prior to coating to increase the wetting characteristics of methanol on the substrate. These included washing with sulfuric acid, flame treatment, soaking in bleach, and coronal discharge. It was empirically determined that the coronal discharge treatment had the greatest effect on increasing the wetting of the coating. Figures 3-8 show the results of spray coating alignment layer in methanol onto glass after various treatments.



Figure 3 - Flame treatment, glass, 10x



Figure 4 - Bleach soak, glass, 10x

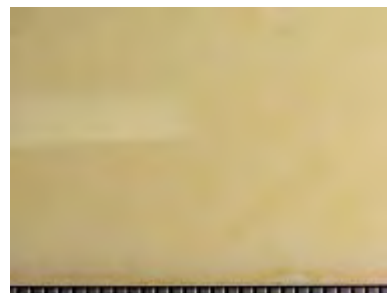


Figure 5 - Corona discharge, glass, 10x



Figure 6 - Flame treatment, glass, 56x



Figure 7 - Bleach soak, glass, 56x

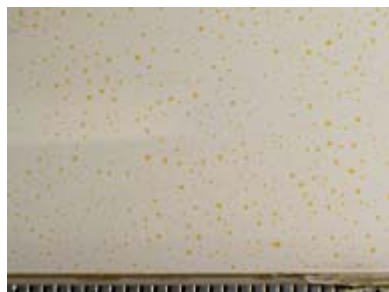


Figure 8 - Corona discharge, glass, 56x

A uniform thin film was achieved on glass after the corona treatment. The treatment involved cleaning the glass normally, and then holding a corona discharge device roughly 3 cm above the surface and sweeping over the surface. Spray coating followed immediately after treatment. The spray coating parameters used to get the uniform thin film on glass were substrate temperature: 30 °C, mass flow rate: 1 mL/min, z distance from substrate: 141 mm, air pressure: 20 psi, gantry scan speed: 30 mm/s, and corona discharge: 2x sweep. The scale in the 10x images is 0.5 mm/division. Results were tested and verified to be reproducible.

Encouraged by the success of the corona discharge surface treatment, we began to study corona discharge on polycarbonate while keeping all other coating conditions the same. The hypothesis was that if the only difference is in the surface morphology and surface energy, then a uniform coating should be achievable with the appropriate surface treatment. The only difference in the cleaning procedure for polycarbonate vs. glass was an acetone sonication wash instead of DI water sonication wash. A baseline HCPC plaque was spray coated with an AZB alignment layer.

Another experiment was conducted with the exact same conditions as those used to produce the uniform thin film on glass, with two sweeps of the corona discharge onto the HCPC plaques. There was no visible change in the coating, so the number of sweeps was increased to six. The alignment layer in methanol wet the surface significantly better with six sweeps of the corona discharge, and a uniform thin film was achieved. The spray coating parameters used to get the uniform thin film on glass were substrate temperature: 30 °C, mass flow rate: 1 mL/min, z distance from substrate: 141 mm, air pressure: 20 psi, gantry scan speed: 30 mm/s, and corona discharge: 6x sweep. The scale in the 10x images is 0.5 mm/division. Results were tested and verified to be reproducible. Figures 9-14 show the results of the corona treatment on HCPC.



**Figure 9 - No wash, hardcoated polycarbonate, 10x**

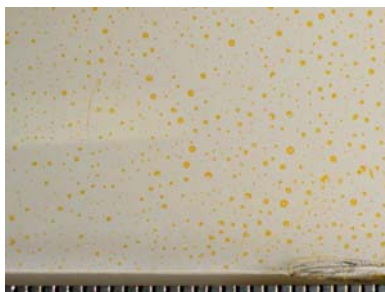


**Figure 10 - Corona discharge, HCPC, two sweeps, 10x**



**Figure 11 - Corona discharge, HCPC, six sweeps, 10x**

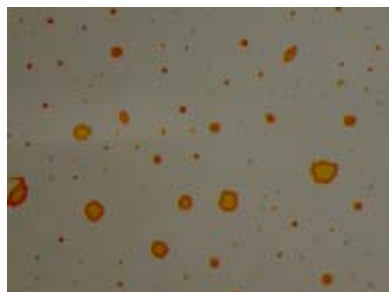


**Figure 12 - No wash, HCPC, 56x**

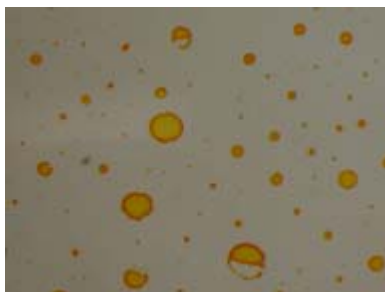


**Figure 13 - Corona discharge, HCPC, two sweeps, 56x**



**Figure 14 - Corona discharge, HCPC, six sweeps, 56x**

The change in surface energy caused by corona discharge clearly resulted in a change in the coating uniformity. Corona discharge was generated using a Tesla coil and produced filaments. These ‘sparks’ are channels of high energy flux, and are usually called streamers. They vary in size and are considered to provide a good surface treatment to improve adhesion between plastics and hydrophilic coatings.

#### 2.3.1.2 Corona Discharge Effect on Ballistics

A corona discharge was used to treat the surface of the polycarbonate plaques by sweeping the plaques under the device held in place with a lab stand. The corona discharge device uses a transformer to create very high voltages (10-40kV) at low current along a thin conducting plasma filament. The corona discharge is considered good treatment for interaction between plastics and hydrophilic coatings. The charged surface creates favorable conditions for wetting of AZB. In Figures 15-17, three HCPC lenses were washed identically. The control had no corona treatment; the second had a minimal treatment, and the third had the correct treatment of six sweeps.

Ballistic properties of coronal treated polycarbonate were tested. A control Saw Fly lens was not treated with coronal discharge, and five additional Saw Fly lenses were treated with corona discharge at various conditions. These conditions were: two passes of corona, six passes of corona, 15 s of corona, 30 s of corona, and 45 s of corona. The most extreme corona treatment represented a nearly 10x greater dosage of energy than was used during the surface treatment stage for AZB adhesion promotion. Samples were then shot with 0.15 caliber fragment simulating projectiles, with an average velocity of 650 ft per second. The substrates were then mounted in the microscope to allow for analysis in transmitted and reflected light.

Each sample was observed in the same fashion and exhibited the same type of ductile behavior, which was consistent with the expected ballistics response of the device. Figures 18-20 show high zoom (40x) images of the impact zones of Figures 15-17. The scale bar on the bottom right hand side is equal to 100  $\mu$ m. On the inside, away from impact, the deformation included a shattered pattern within the impact zone, and spider cracks propagating from the impact center outward. The spider cracks traced the contour of the deformed area at the edge and traveled approximately 300  $\mu$ m away from the crater. On the impact side, the impact center exhibited a similar shattering pattern as the back; however, the surface near the impact site contained a handful of concentric cracks in the hard coating relative to the impact center near the edge of the impact. The concentric cracks were tightly spaced and contained within only 100s of microns from the crater edge.



**Figure 15 - No corona**



**Figure 16 - Six pass corona**



**Figure 17 - 45 s corona**

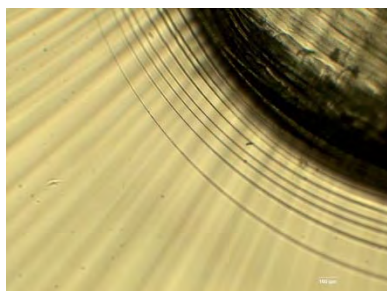


**Figure 18 - No corona, zoom view**

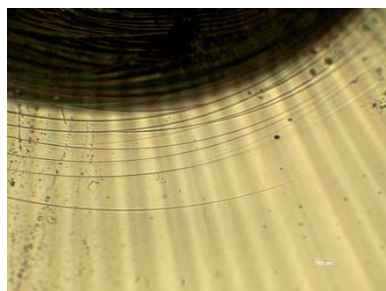


**Figure 19 - Six pass corona, zoom view**

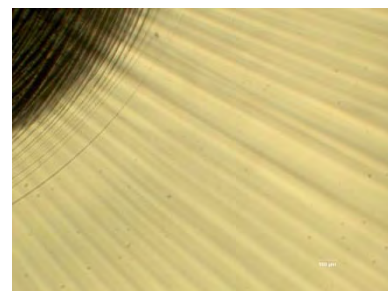


**Figure 20 - 45 s corona, zoom view**

All samples responded with nearly identical hard-coat crack patterns (inside and out) and passed the ballistics test without issue.

### 2.3.1.3 AZB Thin Film Process Improvements

We previously described conditions to produce the AZB thin films; they were: deposition temperature: 30 °C, mass flow rate: 1 mL/min, z-distance from substrate: 141 mm, air pressure: 20 psi, gantry scan speed: 30 mm/s, and corona discharge: 6x sweep. The film was practically



uniform, but it was colored yellow (indicating that the film was too thick) and its measured thickness was ~90 nm. The new set of spray-coating conditions was selected via experimental matrix, which led to producing thinner and more uniform thin films. It was previously thought that a critical requirement for a good AZB film was its smoothness, but it was determined during the meeting that a certain amount of roughness on the surface could be acceptable. This is important, because the ultrasonic spray coating technique necessarily results in a somewhat rough surface due the combination of the atomization mechanism, droplet impact mechanics and wettability of the material being spray coated. It is Revision's opinion that we are at the limit of the spray coater's capability of applying a uniform thin film of AZB. Likewise, it was Beam Engineering's opinion that the AZB layer with minor roughness would be acceptable for the irradiation process. Samples spray coated with AZB using the new set of parameters, subsequently irradiated, and spin coated with LC did indeed show a grating, thereby proving the new AZB coating conditions led to creating a viable thin film. LC layer deposited on AZB coated polycarbonate substrates showed local dewetting spots with greater frequency than on glass.

Figures 21-23 show AZB with improving surface roughness, indicated by a reduction in hills and bumps. The improvements were made possible with proper choice of spray coating variables. Figure 24 and Figure 25 show LC spin coated onto spray coated AZB on glass with grating present. These images indicate that AZB doesn't need to be perfectly uniform to produce a grating under irradiation. Figure 26 shows AZB spray coated onto polycarbonate with LC spin coated and grating present. Local dewetting was significant.



**Figure 21 - AZB poor coating with rough surface**



**Figure 22 - AZB with smoother surface**



**Figure 23 - AZB with smoothest surface**

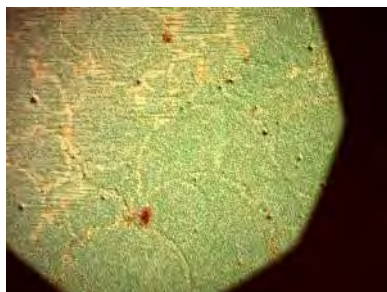


**Figure 24 - AZB/Grating/LC on polycarbonate under differential interference contrast (DIC) illumination**

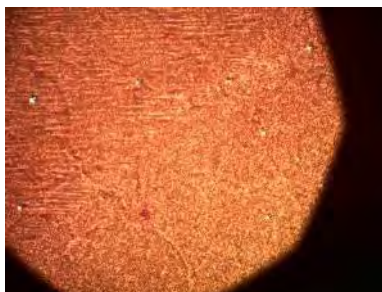


**Figure 25 - AZB/Grating/LC on polycarbonate under DIC**

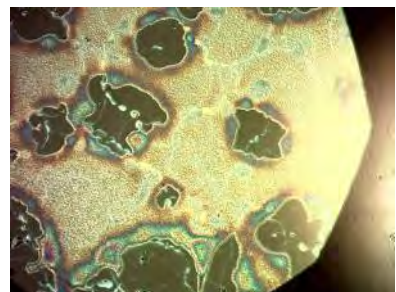


**Figure 26 - Local Dewetting on polycarbonate with grating visible**

#### 2.3.1.4 LC Deposition

The LC has a strong tendency toward dewetting in the current system. A droplet of LC applied onto a thin film of AZB will immediately bead up upon itself. This fundamental chemical incompatibility between the AZB and LC layers drove a significant amount of research effort at Revision during Phase 1 of the UCHET program. Research efforts included a full parameter space matrix to determine the optimal conditions, experiments with changing solvents, temperatures, ultrasonic power levels, and an on-site visit to USI in Haverhill, Massachusetts to see if the manufacturer of the ultrasonic coating system used in UCHET could coat the LC onto the AZB. In each case, a uniform thin film that covers the full area of the plaque was unachievable. A single strip of coating, deposited in a single pass of the spray coater, was possible. It is Revision's opinion that this incompatibility can be solved by selecting coating solvents that are appropriate for the dynamics of spray coating environment.

LC (~1% in cyclopentanone and other solvents) was loaded into the spray coater with a dilution of 1:3 in cyclopentanone. The coating conditions used were: flow rate = 0.5 mL/min, pressure = 60 psi, height = 30 mm, gantry speed = 40 mm/s, temperature = 50 °C, ultrasonic power = one above lowest setting. A 1 cm<sup>2</sup> area was masked off, and a single line of coating was sprayed onto the substrate.

There are a large variety of interacting parameters that exist with the spray coating technique which can affect the quality of a spray coated film, including:

- Height of coating nozzle away from substrate
- Speed to jog gantry
- Air pressure
- Concentration
- Temperature of fluid stream or substrate

#### **Experimental Design**

We created a factorial experimental design to understand how each of the parameters listed above interact with each other in a spray coating process. We ranked the process parameters in order of what we thought had the most effect to the least effect on the coating. Our initial hypothesis was based primarily on spray coating tests of LC performed earlier, where we determined that drying and evaporation were the most important factors. Once again, temperature, height away from substrate, and flow rate were chosen as the most important contributors to uniform film formation, as shown in Table 2.

Table 2 - LC test matrix

Experiment Set	Substrate	Spray Solution	Substrate cleaning/Surface treatment	Spray Parameters and Substrate Temperature
A	Glass	1% in Cyclopentanone	None or cleaning treatment	TBD
B	Glass	0.5% in Cyclopentanone	None or cleaning treatment	TBD
Flow (mL/min)	Temp (°C)	Distance (mm)	Pressure (psi)	Scan (mm/s)
0.31	25	40	20	10/40/100
			40	10/40/100
			60	10/40/100
		80	20	10/40/100
			40	10/40/100
			60	10/40/100
		120	20	10/40/100
			40	10/40/100
			60	10/40/100
	65	40	20	10/40/100
			40	10/40/100
			60	10/40/100
		80	20	10/40/100
			40	10/40/100
			60	10/40/100
		120	20	10/40/100
			40	10/40/100
			60	10/40/100
	95	40	20	10/40/100
			40	10/40/100
			60	10/40/100
		80	20	10/40/100
			40	10/40/100
			60	10/40/100
		120	20	10/40/100
			40	10/40/100
			60	10/40/100

The experiment was specifically about the relationship between spray coating parameters and the quality of an LC thin film on an AZB thin film. The substrates we used were glass 1 x 1 inch substrates. The coating solutions included: 1% LC by weight in cyclopentanone, filtered with 0.45  $\mu\text{m}$  syringe filter; 0.5% LC by weight in cyclopentanone, filtered with 0.45  $\mu\text{m}$  syringe filter. For the case of untreated glass, we sonicated substrate and washed with DI water and dried

with N<sub>2</sub>. For the cleaning treatment case on glass, we sonicated the substrate in soap and isopropanol, and dried with N<sub>2</sub>.

Glass slides were corona treated to promote AZB adhesion and spin coated with 250  $\mu$ L AZB for 30 s at 3000 rpm. The slides were then irradiated with 0.06 J/cm<sup>2</sup> to print the grating pattern. Finally, the substrates were spray coated with LC and cured.

Note that we also performed a low temperature test outside of the test matrix, in which we followed the cleaning procedure listed above. Low temperature was achieved by cooling a block of aluminum to a temperature of 0 °C and placing the substrate on the aluminum block prior to coating. For the low temperature test, we used 0.5% LC by weight, filtered with 0.45  $\mu$ m syringe filter, with m=0.31 mL/min; z=40, 80 mm; P=20, 40 psi; v=20 mm/s.

#### 2.3.1.5 Crystallization Defects and Local Dewetting at Room Temperature

Two main issues with regard to the LC coating were crystallization and local dewetting, both of which occurred quickly after the LC was coated onto the substrate. LC began to crystalize at certain spots, which acted as nucleation sites within tens of seconds after landing on the substrate. After a few crystals formed, they tended to propagate through the film. The crystallization process was retarded with an immediate UV-cure under nitrogen air flow. Fast crystallization of a wet LC film under atmospheric conditions made observation difficult. Crystallization was minimized with immediate curing, but has yet to be completely avoided in samples. It is important to note that crystallization of the LC film was observed nearly immediately following the spray coating process, which typically yields a relatively wet film. It did not occur immediately in spin coating of LC onto AZB, which indicates that crystallization is at least partially related to a time-dependent drying phenomenon. Spin coating resulted in a film that was almost immediately dried after deposition of coating, due to the high rate of forced convective heat and mass transfer out of the substrate as it revolves. However, crystallization had been observed in spin coated LC on AZB that was uncured and left exposed to the environment for roughly 9 h.

Figures 27-32 represent sections of typical LC films coated at standard conditions. Figure 27 presents a uniform section of LC, and Figure 28 shows a uniform section of an LC thin film with surface waves. Figure 29 presents typical dewetting spots in a film. LC was measured to be between 2.5  $\mu$ m to 10  $\mu$ m, depending on coating conditions. Thick LC, defined as having film thickness >3.5  $\mu$ m, exhibited at least three types of crystallizations. The first type of crystallization was nucleated at surface defects, either by scratches made before coating or by dust, and grew radially from a point. Figure 30 presents this type of radially grown crystallization defect, and Figure 31 presents the defect at higher magnification. Figure 32 is a blank reference image for comparison with coated slides. The second type was less ordered and feather-like. The third type had a spherulitic structure and grows between the large crystals and the feather-like crystals. Crystallization tended to propagate through an uncured film within minutes of spray coating deposition. Various types of lighting help visualize the defects.



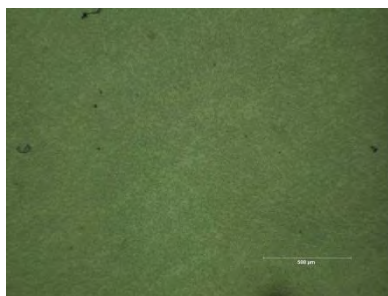


**Figure 27 - LC on AZB**



**Figure 28 - LC on AZB, wavy**

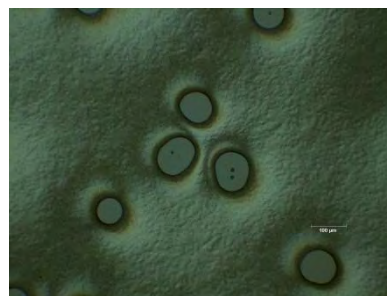


**Figure 29 - LC on AZB, local dewetting**



**Figure 30 - Solid crystal nucleation sites**

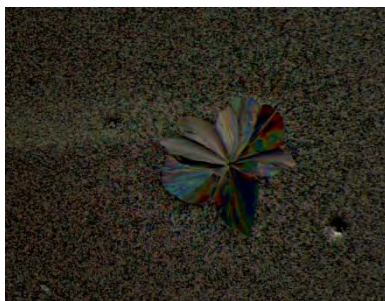


**Figure 31 - Crystal, high magnification**



**Figure 32 - Reference blank**

Figures 33-38 present defects of various morphology, including radial nucleation and growth, feather-like crystals, spherulitic structures, local dewetting, and crystalline grain boundaries.

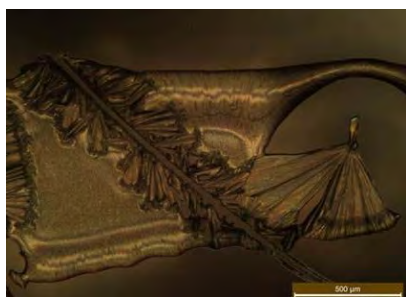


**Figure 33 - Thick LC film with crystallization**

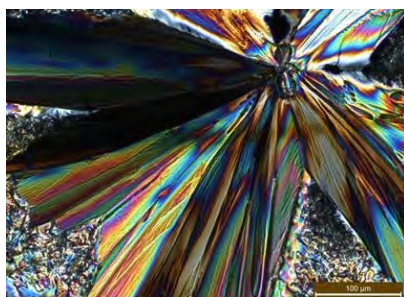


**Figure 34 - Crystallization, polarized light**

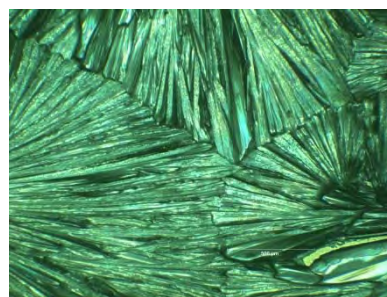


**Figure 35 - Crystallization with boundaries**



**Figure 36 - Feather-like crystals**

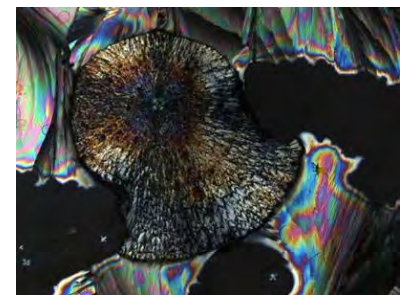


**Figure 37 - Spherulitic structure, polarized light**

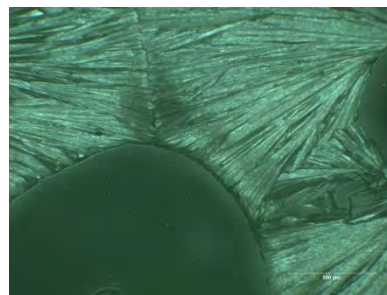


**Figure 38 - Crystals, boundaries, and local dewetting region**

Figure 39 shows a panoramic view helps visualize the level of defects observed across a substrate surface that was spray coated, uncured, and left to dry at atmospheric temperature and pressure. We observed local dewetting on the far left, and crystallization propagation to the right with various defect morphologies scatters throughout the field.



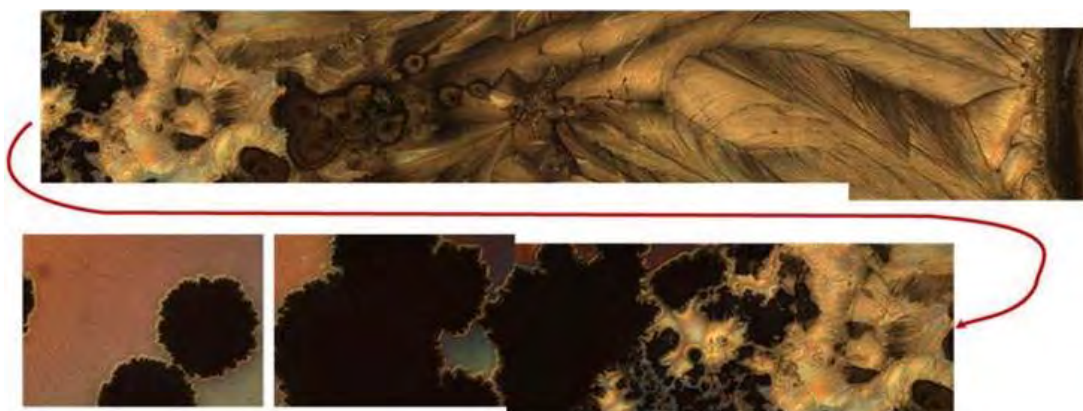


**Figure 39 - Panoramic view of crystal growth**

### 2.3.1.6 High and Low Temperature Tests

We performed a low temperature test, where a block of aluminum was cooled to 0 °C before being placed in the spray chamber to chill the substrate. At low temperature, all three types of macroscopic crystals were observed. Some of the spherulitic-type structures grew as cascades. Figures 40-45 show the various defects. Condensing water damaged the AZB, and did not prevent growth of crystalline defects. We believe that condensing water solvates the AZB, disrupting that layer and creating a less favorable surface for LC interaction.

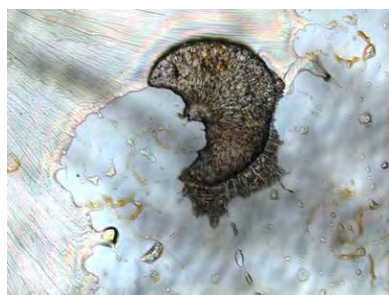


**Figure 40 - Spherulitic structure, low temp**

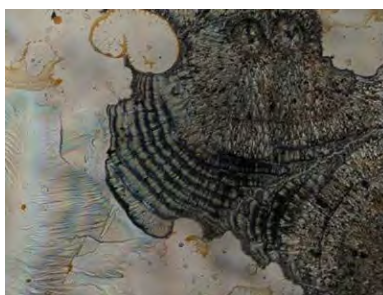


**Figure 41 - Feather-like structures, low temp**



**Figure 42 - Radial crystal growth, low temp**

We also observe feather-like structures that protrude above the surface. It was possible to focus the image at various depths to observe the level of protrusion out of the film. Figure 43-45 show the feather-like structures, observed with crossed polarizers.

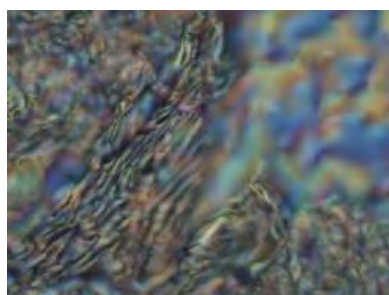


**Figure 43 - Feather-like structures, high-range focus**

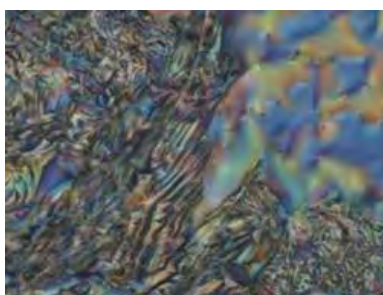


**Figure 44 - Feather-like structure, mid-range focus**

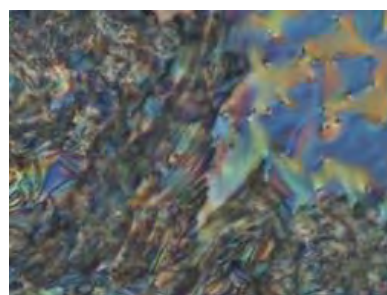


**Figure 45 - Feather-like structure, low-range focus**

The presence of crystals was limited when the LC was coated at room temperature and immediately cured, but local dewetting occurred and disrupted film uniformity. We found that crystallization would still occur on the order of hours in thicker samples, even after curing, over some or all of the substrate.

Figures 46-51 are images of local dewetting in the LC layer. To verify if dewetting takes place at the AZB/LC or AZB/HC interface (in other words, above or below the AZB layer), we exposed the coated samples to water vapor below the dew point, as shown in Figure 48 and Figure 49. AZB is soluble in water, so condensation of water onto the substrate can dissolve the AZB and free the LC coating, as observed in Figure 49. We concluded that dewetting occurred between the LC and AZB layer; the latter remained intact in the dewetted zone and it was removed during water condensation (compare Figure 48, Figure 49, and Figure 51). Spots in the center of dewetting regions, as seen in Figures 46-51, indicate contamination, which was possibly the cause of dewetting by the induction of a surface tension gradient at those points in the field. The contamination might be dirt, or it might be gas trapped in the coating during the spray process where nitrogen was used to direct the coating microdroplets to the substrate. Energy-dispersive x-ray spectroscopy should be used to analyze the dewetting zones to obtain conclusive data.

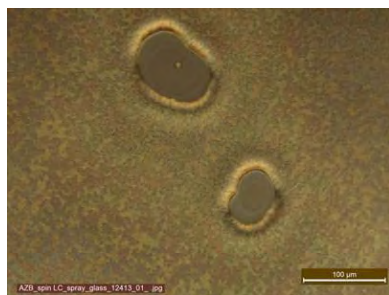


**Figure 46 - Local dewetting**



**Figure 47 - Local dewetting, zoom**

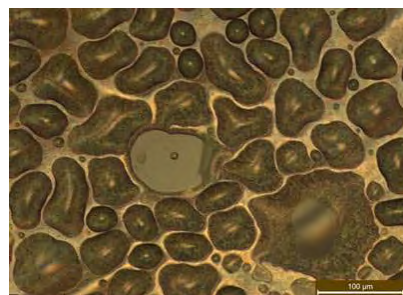


**Figure 48 - Water condensation on AZB/LC**

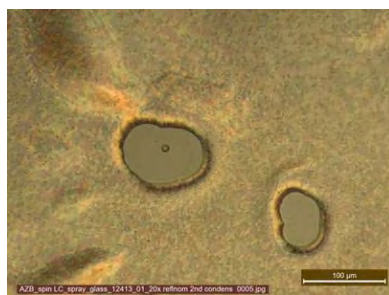


**Figure 49 - Local dewetting, wavy surface after exposure to condensed water**

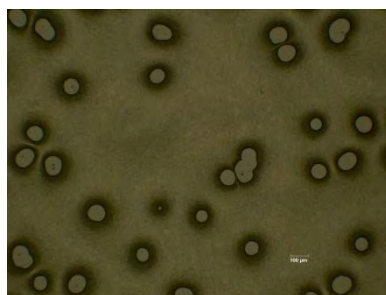


**Figure 50 - Dewetting, low magnification**



**Figure 51 - Dewetting, high magnification**

Dewetting was also triggered in our high temperature tests (95 °C) and appeared worse than at room temperature, where dewetting occurred peripherally on the substrate rather than throughout the film. Figure 52 and Figure 53 show continuous coating with a high number of ‘lakes’ and ‘islands,’ and Figure 54 shows a crystal and dewetting zone with ‘islands.’

The results of our experiments with exposure to low temperature and water vapor shine some light on the required quality of the intended product – eyewear lenses. The top surface of the lens having the waveplate must be coated with a defect-free hard coating to protect the AZB and LC



materials from the environment. Although the typical hard-coat protects the underlying materials from water, it is very difficult to produce completely free of micrometer and sub-micrometer pinholes. This problem is well known in the barrier coating industry and has a significant impact on the design of plastic organic light emitting diode displays and flexible photovoltaic devices.

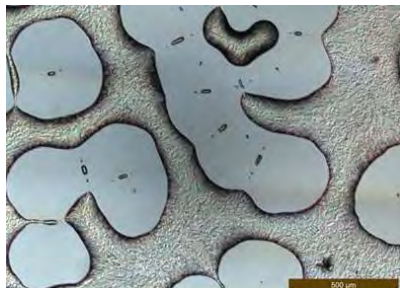


Figure 52 - High temp dewetting, 'lakes'

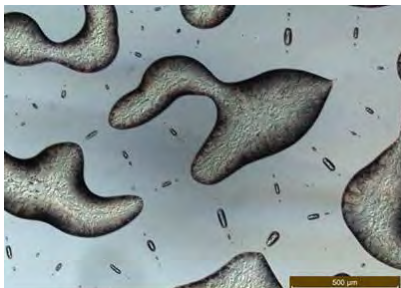


Figure 53 - High temp dewetting, 'islands'



Figure 54 - High temp dewetting, crystallization boundary

#### 2.3.1.7 Mixed Solvents

Spray coating of the LC polymer monomer onto thin AZB films was always characterized by significant dewetting and hence unacceptable polymer films. This was verified at the USI, where the applications engineers who are expert spray coaters could not get a uniform thin film of LC to completely cover the AZB. The exception to this was when polymer films were sprayed in “single pass” mode onto heated AZB substrates, as described in Monthly Report 9. All LC monomer spray coating materials supplied by Beam Engineering were diluted in cyclopentanone and other unknown solvents. Cyclopentanone is a relatively polar solvent, and it was supposed that less polar solvents would reduce surface dewetting during spray coating. This idea was evaluated by observing the contact angle of several solvents on AZB films and comparing the angles to that of cyclopentanone. Two very non-polar solvents exhibited reduced contact angles: toluene and xylene. The xylene used in our studies was technical grade and was a mixture of ortho, meta and para isomers.

At the time these experiments were being conducted, a new batch of LC monomer was received from Beam Engineering to replace the dwindling supply of old LC. This material was very different in appearance from the original monomer in that it was a white colloidal mixture with higher viscosity than typical. It also did not have the characteristic odor of cyclopentanone. Both the old and new LC monomer materials were used to prepare lower polarity mixed solvent solutions. 1 mL of old monomer was added to 5 mL of toluene and xylene in separate 20 mL vials. These solutions were shaken and resulted in a single phase, clear, homogeneous liquid. The new monomer was initially stirred with a magnetic stirrer for approximately 5 min. Then 1 mL of the mixture was added to 5 mL of toluene and xylene in two separate 20 mL vials. These solutions were also single phase, clear, homogeneous liquids.

Each of the four resultant solutions was spin coated onto previously prepared AZB coated substrates, resulting in satisfactory uniform thin films. These films were then polymerized with UV light as previously described. Films prepared from the original monomer formed stable films after irradiation. The films from the new monomer did not appear to properly polymerize as the films began to form crystalline patterns only a few minutes after spin coating. The crystallization

eventually covered the entire coated surface. Deposition of new monomer coatings were repeated with the same effect. In each case, the monomer was coated and cured in typical fashion. The new monomer does not crystallize; therefore, it is not useful for the project.

The old monomer solutions in toluene and xylene were then used in the USI spray coater to prepare thin polymer films on AZB substrates. For both solvents, and under a wide range of spray conditions, high quality coatings could not be achieved in “multi-pass” mode. Several films were considered an improvement, but the overall quality was not acceptable for preparing the desired polarization gratings.

Additional mixed solvent experiments were conducted using 10% (v/v) of methoxy - 2- propanol in xylene. These solutions exhibited good wetting characteristics; however, the solvent mixture appeared to interfere with UV polymerization. Thin films of these materials eventually crystallized after curing, similar to the new monomers.

#### 2.3.1.8 Spray Coating with Lower Boiling Point Solvents

Several researchers have published work showing that the rate of solvent evaporation from the coating can be important in controlling surface dewetting. In many cases, solvents that evaporate more rapidly were shown to improve spray coating of polymeric materials. To explore this with our LC, methyl ethyl ketone (MEK) was chosen as an alternative solvent. The boiling point of MEK is 79.6 °C and the solvent is compatible with spray or spin coated thin films of the AZB material.

Solvent exchange was initially attempted by evaporating cyclopentanone from the LC on a hot plate set at 80 °C. The LC solutions were taken to dryness and reconstituted in MEK. The resultant solution contained large amounts of undissolved material that suggested that the LC had thermally polymerized to some degree during the heated evaporation.

An alternative method that was inherently low temperature was devised. 1 mL of LC was transferred to a 20 mL glass vial. The solvent was evaporated under a steady stream of nitrogen (30 mL/min) until the polymer monomer crystallized and there were no visible traces of the liquid solvent. The vial remained noticeably cold during the evaporation process. The process is shown in Figure 55.

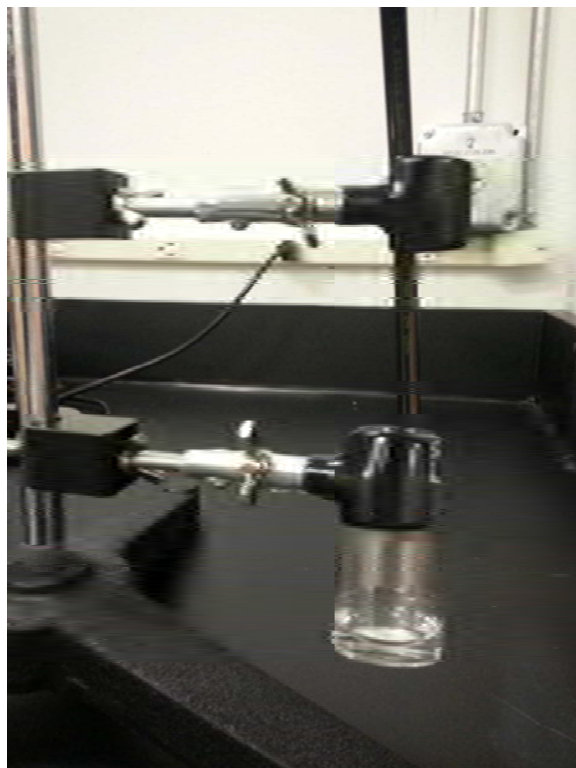


**Figure 55 - LC solvent exchange facilitated by evaporation with nitrogen stream**

The resultant material was reconstituted into 1 mL of MEK with light mixing. After approximately 5 min the quiescent solution was visually examined and found to be clear with a very small amount of white long material suspended in the MEK. The suspended material was easily removed via filtration through a 2  $\mu$ m filter. Several 5 mL batches of solvent exchanged LC were prepared for use with spray coating system.

The LC in MEK was spin coated (1:5 dilution in MEK, 300  $\mu$ m, 30 s) onto glass slides that had been ultrasonically washed with propanol and spin coated with AZB (PAAD-72, 1:3 in methanol, 300  $\mu$ m, 3000 rpm, 30 s). The resulting films were uniform, but dewetting was observed. The films looked qualitatively worse than films spin coated with LC in cyclopentanone. A possible reason for this is differences in solubility of LC in MEK vs. cyclopentanone. Further tests were carried out with the spray coater. The LC in MEK was spray coated at room temperature onto HCPC slides that had been spin coated with AZB. Temperature was held constant. Flow rates varied from 0.31 mL/min to 2.5 mL/min. Distances varied from 30 mm to 120 mm. Pressure was varied from 20 psi to 60 psi. Speed of gantry movement was varied from 20 mm/s to 80 mm/s. In all cases, the dewetting was typical of spray coating LC at room temperature. Figures 56-58 show representative films made by spin and spray coating LC in MEK.



**Figure 56 - LC in MEK, spin coated onto AZB spin coated glass; with diffraction grating.**



**Figure 57 - Local dewetting of LC in MEK, spray coated onto spin coated AZB spin coated HCPC.**

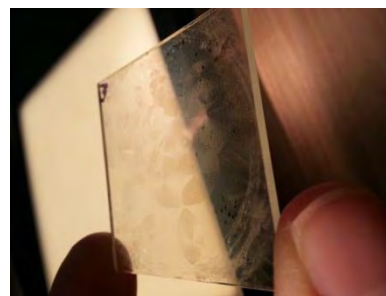


**Figure 58 - Crystallization of spin coated LC in MEK over a period of 24 hours**

LC in MEK was not spray coated onto heated substrates, as the heated substrate experiments and improvements they exhibited were discovered several weeks after the MEK experiments occurred. By that time, LC in cyclopentanone had produced good films when deposited onto a heated substrate and the MEK re-solvation experiments had been postponed.

#### 2.3.1.9 Spray Coating with Elevated Substrate Temperature

Due to the difficulties spray coating LC in cyclopentanone and MEK, the coating apparatus was modified to incorporate variable heating of the substrates. Substrate heating has been successfully used for conformal coatings in microelectronics industry (Solar Energy, Materials, & Solar Cells; 2012, 107, 292–297), and has been used in previous Revision projects to improve wetting of coatings deposited with the spray coater. Initial experiments were performed using LC at 1% in cyclopentanone with a substrate temperature of 25 °C. Gantry speed was fixed at 40 mm/s for glass and 80 mm/s for HCPC, as seen in Table 3.

**Table 3 - Experimental design for LC spray coat test, with temperature as dependent variable.**

<b>Flow</b> [mL/min]	<b>Distance</b> [mm]	<b>Pressure</b> [psi]	<b>Temp</b> [°C]	<b>Passes</b> (# of passes, lines or S pattern)
0.5	30	30	30	1/2/S
			50	1/2/S
			70	1/2/S
		60	30	1/2/S
			50	1/2/S
			70	1/2/S
	45	30	30	1/2/S
			50	1/2/S
			70	1/2/S
		60	30	1/2/S
			50	1/2/S
			70	1/2/S

To simplify the spray coating process, initial coatings with substrate heating were prepared with a single pass of the spray head over the target substrate. Table 1 shows the experimental design used. These conditions produced the first non-dewetting spray coated LC film on a spin coated AZB substrate. 1 x 1 inch glass slides were prepared by sonication wash in propanol and dried with nitrogen. The slides were then spin coated with AZB (PAAD-72, 1:3 dilution, 300  $\mu$ m aliquot, 3000 rpm, 30 s); irradiated with 442 nm (average power ~15 mW, 45 s); placed on a heated stage (50 °C), and spray coated in a single pass over the substrate (flowrate = 0.5 mL/min, height = 3 cm, pressure = 60 psi, gantry speed = 40 mm/s). A uniform thin film was achieved with minimal dewetting. See Figures 59-61.



**Figure 59 - LC spray coated onto spin coated AZB glass, center area.**

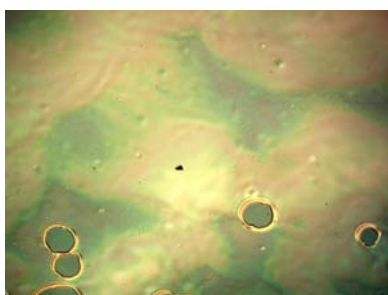


**Figure 60 - LC spray coated onto spin coated AZB glass, boundary area.**



**Figure 61 - Macroscopic view of spray coat pattern on glass. Transparent area was irradiated. Boundary area observable.**

The process was then applied to a HCPC plaque. 2 x 3 inch HCPC plaques were cleaned by sonication wash in propanol and dried with nitrogen. The slides were then spin coated with AZB



(PAAD-72, 1:3 dilution, 500  $\mu\text{m}$  aliquot, 3000 rpm, 30 s spin); irradiated with 442 nm polarized light (average power  $\sim 15$  mW, 45 s); placed on a heated stage (50  $^{\circ}\text{C}$ ), and spray coated in a single line over the substrate (flow rate = 0.5 mL/min, height = 3 cm, pressure = 60 psi, gantry speed = 80 mm/s). Again, a uniform thin film was achieved with minimal dewetting, as shown in Figure 62. Figure 63 shows the characteristic dewetting of the boundary region. LC in cyclopentanone did not evaporate as fast off the surface of the AZB coated plaque as it did off the AZB coated glass slide. This required a slight modification to the spray coating parameters to reduce the amount of material on the substrate surface. Figure 64 is a macroscopic view of the HCPC slide. Note the pooling of the coating at the top of the slide. This unexplained pooling occurred at the start position of the coating on the substrate. It was observed on both glass and HCPC substrates when spray coated with LC, and can be easily observed in Figure 61 as well. It can be mitigated, but not removed, from a coating by reducing the mass flow rate.



**Figure 62 - LC spray coated onto spin coated AZB HCPC, center area.**

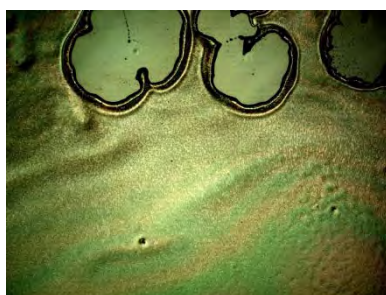


**Figure 63 - LC spray coated onto spin coated AZB HCPC, boundary area local dewetting.**



**Figure 64 - Macroscopic view of LC spray coat pattern on HCPC. Boundary area observable. Pooling of coating observable at start position.**

Multiple passes of the spray coater using a continuous S pattern were attempted next, as shown in Figures 65-66. Interestingly, a uniform coating was unachievable using this method, as evidenced in Figure 66. It appears that the fan spray pattern's boundary solvates the previously deposited film, disrupting the coating and causing dewetting. In another test, two parallel lines were coated a set distance from one another with a set amount of time between coatings. Once the films approached a critical distance of  $\sim 1.0$  cm, the solvent from the coating of the second pass would overlay onto the coating of the first pass; disruption of the film was observed. Figure 65 shows a typical result of the parallel line test. In another test (not shown), a single line coating was deposited, cured, and then over-coated with a second line. In this case, the first line of coating was not disrupted since the film had been cross-linked, but the resulting film was opaque and had obviously high haze.

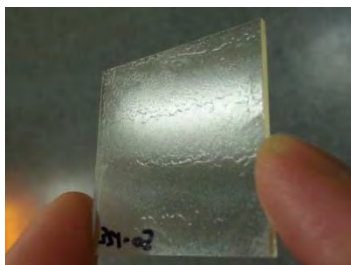


**Figure 65 - Parallel line LC spray coating. Boundary of spray pattern visible.**



**Figure 66 - Serpentine LC spray coating. Boundary not visible. Obvious disruption of film.**



We spray coated LC films onto heated glass and polycarbonate plaques that had been spray coated with AZB, after verifying the viability of the heating process to promote wetting. We have previously spray coated AZB onto glass and HCPC plaques, and utilized the same AZB spray coating conditions as reported in Progress Report #8. The LC was spray coated in the same conditions as listed above, and the results are shown in Figure 67-70. Figure 67 shows the LC film that was spray coated onto HCPC in the center region. Figure 68 and Figure 71 show the characteristic boundary dewetting. Figure 70 and Figure 72 show evidence of a good AZB film deposited by spray coating.



Figure 67 - LC spray coated onto AZB spray coated HCPC, center region.



Figure 68 - LC spray coated onto AZB spray coated HCPC, boundary region.

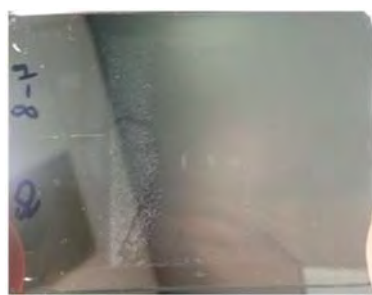


Figure 69 - Macroscopic view of LC spray coating.



Figure 70 - AZB spray coated onto HCPC.

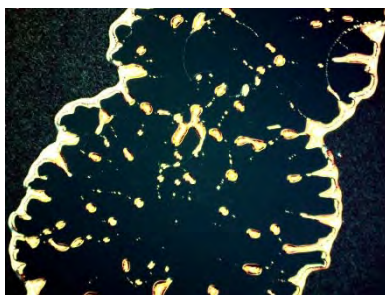


Figure 71 - Local dewetting of spray coated LC on spray coated AZB HCPC.

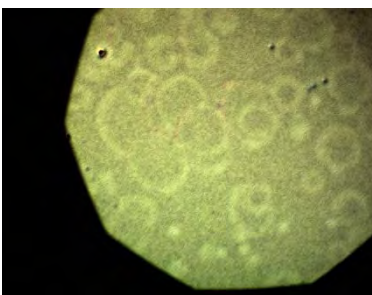


Figure 72 - Spray coated LC on spray coated AZB.

Again, the LC would form a thin film as a single strip of coating, but when attempting the continuous coating serpentine pattern or parallel line tests, the film was destroyed. A properly deposited strip of coating has multiple regions, including the central region and the boundary regions. The central region is where the coating is uniform and continuous. The boundary region is where the coating strip terminates, and typically receives 25-50% of the coating volume in the next pass of the spray coater. Under a single pass, the width of a strip of coating is roughly  $1.7 \pm 0.3$  cm, depending on the thickness of the boundary region (which is non-uniform in position). See Figure 73 for a detailed view of these regions. The average width of coating is a function of the distance away from the substrate, the mass flow rate of the coating, and the evaporation rate of the film solvent(s). The LC film has an optimal distance required for spray coating; too far from the substrate (greater than 4.0 cm), and the film will not form at all; too close to the substrate (less than 3.0 cm), and then air pressure from the nozzle will blow the substrate off its chuck or create pooling and local dewetting of the coating. The mass flow rate was optimized at 0.5 mL/min, and the distance away from the substrate is essentially fixed; thus the coating strip width was essentially fixed at roughly 1.7 cm.

This result is very important to note, as it is nearly impossible to coat a large surface area using a single line of coating in a spray coater. The spray coater presently used, by its design, deposits coating in roughly a Gaussian distribution of droplet number density across the width of spray. The central droplets coalesce, but the boundary droplets do not. The coating necessarily must overlap at the boundaries to create a uniform film. However, non-simultaneously deposited coating overlap has been experimentally shown to disrupt the film, as one line of coating deposited at  $t=0$  dries and then is re-solvated by its neighbor deposited at  $t=t_1$ . Figure 74 is a larger version of Figure 65, detailing the dimensions of the boundary and central regions typical of the line coating. One proposed solution is a multi-nozzle spray coater that deposits  $n$  lines of coating simultaneously. If  $n$  lines are deposited at the same time, then, in theory, the next-neighboring lines will dry at the same time without promoting disruption of the film. A spray coater that could coat a plaque or lens in a single pass is available from USI.

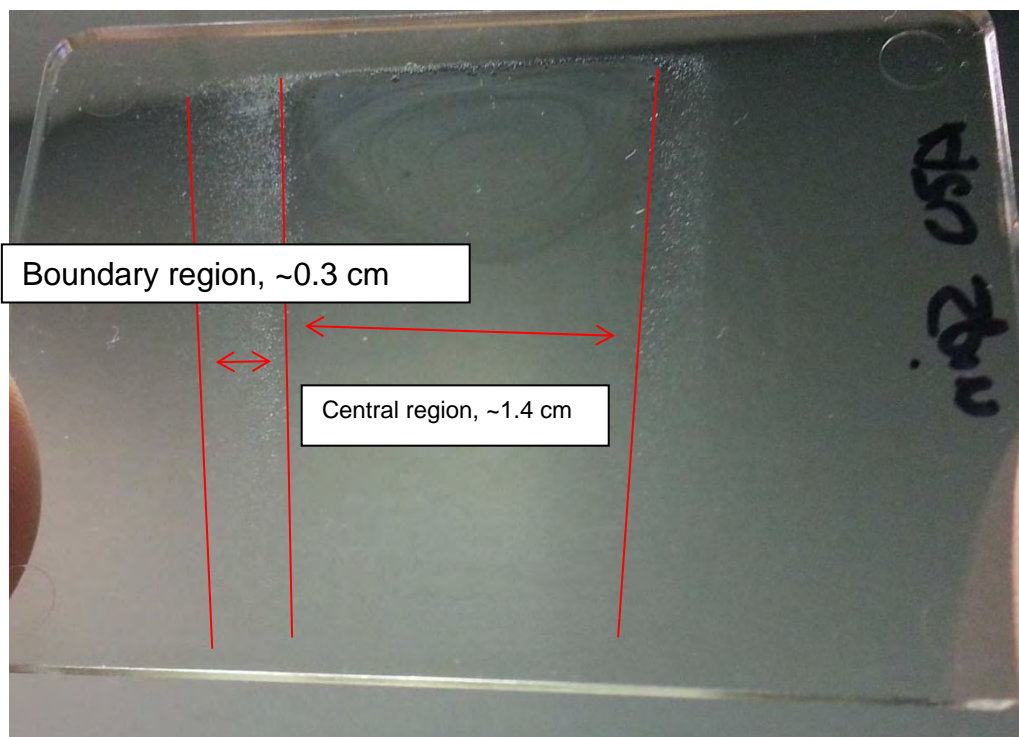


Figure 73 - Central and Boundary regions of spray coated LC

#### 2.3.1.10 Onsite Testing at USI

Ultrasonic Systems is the manufacturer of ultrasonic spray coater machines used in a variety of industrial applications, and Revision is using a USI Prism 300 for the UCHET program. Due to the persistent difficulty of spray coating the LC monomer onto an AZB coated substrate, Revision made an onsite visit to USI in Haverhill, MA. The purpose of this visit was to use USI experience and expertise to eliminate the possibility that there was a machine specific incompatibility with the LC material. The visit was also to have the USI applications engineers make recommendations to help identify parameters that would lead to better LC coatings after observing the physics of the material in their machines.

Several samples were prepared in advance of the trip to USI, including both spin and spray coated AZB in methanol at a 1:5 dilution on glass and HCPC. Both spin and spray coated substrates were treated to 10 sweeps of corona discharge before coating, and the solutions were filtered with 0.45  $\mu\text{m}$  syringe filters before being mixed. Spin coating conditions were: 300  $\mu\text{L}$  material; 3000 rpm, 30 s; material deposited at 500 rpm. The spray coating conditions used were: z height = 120 mm; velocity = 100 mm/s; Pressure = 60 psi; mass flow rate = 0.35 mL/min; serpentine spray pattern; power setting = selector set one below maximum power; temperature = 50 °C. The substrates were not UV irradiated. After deposition, substrates were stored in a nitrogen box until they were packed into air-tight boxes for transport. A 1:3 dilution of the standard Beam Engineering LC material in cyclopentanone was prepared for testing at USI. The LC and cyclopentanone was filtered in 0.45  $\mu\text{m}$  filters prior to mixing, and then prepared via the standard method.

Upon arrival at USI, properties of the materials to be coated (chemical composition, concentration and approximate viscosity) were reviewed. It was noted that the polymer solution was considered “low viscosity” and within the capability of the ultrasonic atomizer of the Prism 300 spray coater. USI also reviewed the typical instrument settings used by Revision when coating in the Essex Junction facility. After this review, the LC material that Revision brought was loaded into the spray coater. The spray coater at USI has had a modification made to the system that enables fairly quick change in atomization power, which enabled broader experimentation than with the fixed atomization power system that comes standard on the USI spray coater. A hot plate was also installed in the spray chamber.

The initial conditions used were set to match the typical conditions used in the UCHET spray coating process at Revision, including: atomization power, flow rates, gantry speed, temperature, pressure, and distance from substrate. The USI factory test system had a useful diagnostics feature where the door interlocks could be defeated for engineering setup and calibration. This enabled a close observation of the mist generated by the nozzle and behavior of the environment surrounding the plume. The first substrate tested to verify the system parameters was a piece of clear Mylar film. The spray coat pattern included a serpentine sweep over an area of 3x10 cm. The initial coating had ideal wetting of the LC material to the surface. The coating was visibly thicker than a coating made with the same parameters on polycarbonate. However, it appeared that too few LC solids were in the coating after the solvent evaporated. The figure below shows the dried coating with overlapped areas achieving sufficient amounts of LC material.

The subsequent tests were all performed upon the AZB coated substrates, and all experienced various degrees of dewetting. The first test was on an AZB coated glass plaque and presented a good coating before the LC film retracted into itself seconds after deposition. This coating is shown in Figure 75. All subsequent tests included progressively worse dewetting, as temperature was increased, and as nozzle power was lowered and raised. Figures 74-77 show different degrees of dewetting on AZB substrates.



Figure 74 - Mylar coated with LC

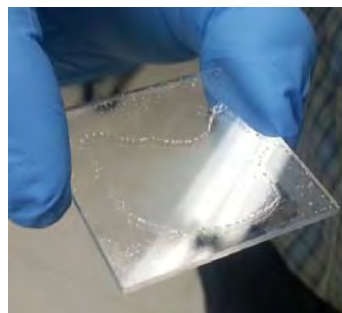


Figure 75 - Glass AZB substrate coated with LC, typical dewetting

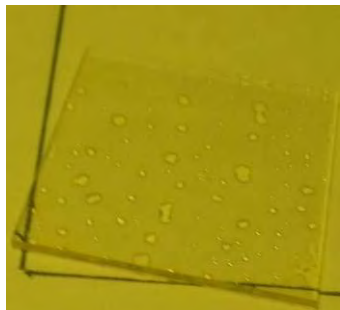


Figure 76 - Glass AZB substrate coated with LC, strong tendency for dewetting

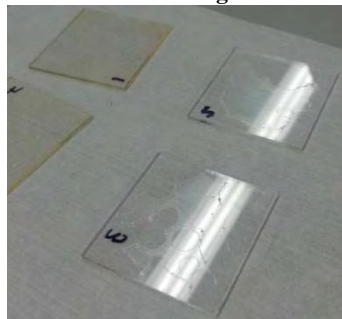


Figure 77 - Glass and PC AZB substrates with LC; different degrees of dewetting

A variety of testing was carried out with different conditions, as listed in Table 4. Some of the warmer temperatures yielded coatings that started to approach the spray results on Mylar, but the underlying incompatibility of the LC and AZB materials quickly became obvious. The USI system was unable to deliver an acceptable thin film of LC on AZB, as the spray coating process was overwhelmed by the incompatibility of the LC layer and the AZB layer surface chemistry. The exception was a sample spray coated onto a non-hardcoated, non-treated polycarbonate plaque without AZB. In this case, a uniform thin film of LC was repeatedly achievable; pinholes in the film were observed.

Table 4 - USI LC spray coating conditions and results

#	Sub	Pres	Power	Distance	Temp	Speed	mL/m	Result
1	Glass	20	Mid	30 mm	20	80	1.0	Good initial, surface retracts
2	Glass	20	Mid	30 mm	20	80	1.0	Center good, surface retracts
3	Glass	20	Low	30 mm	20	80	1.0	Very spotty, dewetting
4	Glass	20	Low	30 mm	20	80	1.0	Very spotty, dewetting
5	Poly	20	High	30 mm	20	80	1.0	Dewetting
6	Poly	20	High	30 mm	20	80	1.0	Dewetting
7	Ploy	20	Mid	30 mm	40	80	1.0	Some OK areas, dewetting
8	Poly	40	Mid	30 mm	40	80	1.0	Very bad, complete dewetting
9	Poly	40	Mid	30 mm	50	80	1.0	Some dewetting
10	Poly (no HC)	40	Mid	30 mm	20	80	1.0	Uniform thin film, pinholes

#### 2.3.1.11 Theoretical Model for the LC Film

Suppose we deposit a LC film on the substrate of a certain thickness and concentration. As the solvents start evaporating, all of the following events happen simultaneously but with different kinetics: the thickness decreases, the concentration increases, the surface temperature slightly decreases, the viscosity increases, and the surface tension of the liquid changes.

At least one of the system components has a strong tendency to crystallize in the form of single crystals, or in the form of semi-crystalline structures. When given a nucleation center and enough time, the crystals start growing. “Crystallization” may also be promoted by shear forces in locally oriented flow, as seen in the crystals on spin-coated, uncured samples.

Assuming that the coating forms a uniform, smooth surface, and assuming that there is a mismatch between the surface free energy of the dry AZB coating and the surface tension of the LC solution, we expect the following points to hold true:

1. If the coating dries very fast, there is no time to form crystalline morphology before the viscosity is very high and actually immobilizes the structure. This can only happen with a very thin, uniform film that is quickly dried.
2. If the coating dries slowly (cold substrate or too thick of a coating), two things may happen: (a) crystallization and (b) dewetting. High temperature accelerates evaporation thus inhibiting crystallization but the same time decreasing viscosity which promotes dewetting.

There are additional confounding factors that are not well understood in our system. For example, the role of air and nitrogen micro-bubbles produced in the liquid coating during spraying is not currently well understood. The bubbles may form by degassing from the liquid or they might be trapped during spraying, and may possibly be the centers of dewetting.

#### 2.3.2 Irradiation System

Output of the 40 mW continuous wave He-Cd gas laser was focused through a 25  $\mu\text{m}$  pinhole using a 16.5 mm focal length microscope objective lens. The pinhole was positioned for maximum light transmission and suppression of Airy diffraction rings. The microscope objective and pinhole are the elements of a spatial filter that improves the uniformity of the laser beam intensity profile. The expanding beam from the pinhole is collimated with 300 mm focal length plano-convex lens positioned 300 mm from the pinhole to create uniform wave-front illumination of the polarization grating master and substrate. For this combination of lenses, the beam diameter is expanded from 1 mm to approximately 2 cm, to fill the area of the polarization grating.

With a direct illumination of the master, the beam polarity is easily matched to the master by witnessing a diffractive spread at long distances on the far laboratory wall. The master is secured within a rotational mount for precise adjustment. These initial adjustments greatly improved the quality of the exposures. While images have been obtained using crude setups (simply placing the master atop the substrate), Revision feels it is possible to maximize the



efficiency of the master by matching the illumination to the master and substrate to ensure a uniform and reproducible image plane.

Applying these changes to the exposure system resulted in dramatic improvements over the previous exposure system. The exposure area on a substrate is now optically clear with significantly reduced haze. Power readings across the diameter of the beam are tighter (~25 mW to ~40 mW). The grating looks objectively better, which is likely due to the combined effect of all three changes to the exposure system. Figures 78-80 show the UCHET device on glass and polycarbonate, with AZB and LC spin coated. Figure 78 and Figure 79 are the same glass sample, rotated 90° to show the grating. Figure 80 is the grating on a polycarbonate plaque.



**Figure 78 - UCHET on glass, new exposure system, 0° rotation**

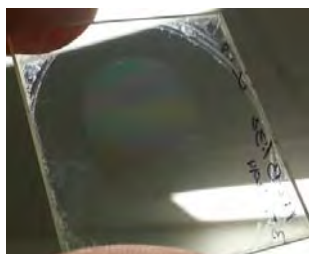


**Figure 79 - UCHET on glass, new exposure system, 90° rotation**



**Figure 80 - UCHET on polycarbonate, new exposure system**

The new irradiation system was tested by spin coating AZB (300  $\mu\text{m}$ , 1:5 dilution in methanol, 30 s @ 3000 rpm) onto glass and polycarbonate slides (ultrasonic washed in methanol,  $\text{N}_2$  dry), irradiation at 442 nm (power~15 mW, 10 s exposure), spin coating LC (500  $\mu\text{m}$ , 1:7 dilution, 30 s @ 3000 rpm), and curing at 365 nm for 120 s with a  $\text{N}_2$  purge. Figure 81-83 show an overview of the new system, including the angle selection master grating jig and rail system for positioning. The significant improvement over previously made devices was immediately apparent, with optically clear substrates in transmitted light and the grating visible at certain angles in reflected light. Shining a 532 nm laser through the grating showed diffraction and reflections that were similar to those shown by the master grating. The LC layer has a thickness of ~0.001 mm which seems to be too thin for effective blocking of 532 nm (Sarik R. Nersisyan, Nelson V. Tabiryan, Diane M. Steeves, and Brian R. Kimball, "The Promise of Diffractive Waveplates," Optics & Photonics News 21(3), 40-45 (2010)). LC thickness can be varied by changing the dilution, thus tuning the film thickness for a particular wavelength.

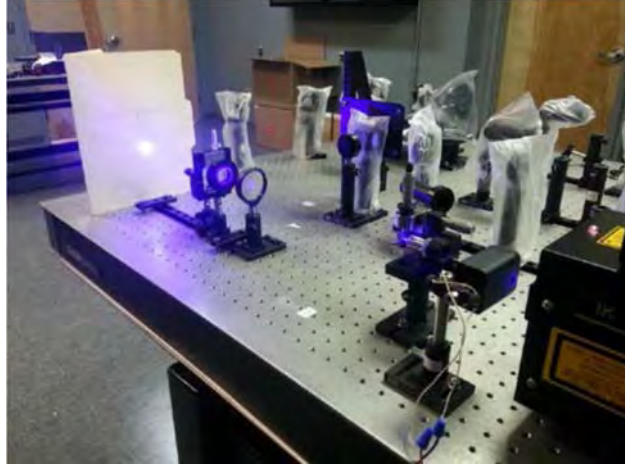


**Figure 81 - Optical Alignment and Collimation**

In addition, specialized stages for positioning glass and polycarbonate substrates were fabricated and placed in line with the collimated beam on an adjustable rail system. The stages have sufficient degrees of freedom to position substrates highly perpendicular to the incident beam by careful alignment of the first surface back- reflection. Average power efflux through the master grating was measured at  $\sim 15 \text{ mW/cm}^2$ , sufficient for irradiation of the AZB alignment layer ( $I=60 \text{ mJ/cm}^2$ ).

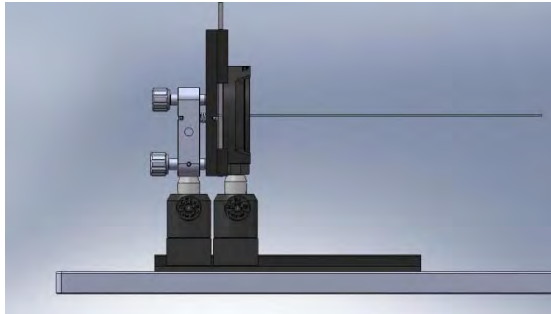


**Figure 82 - Optical fixturing system.**

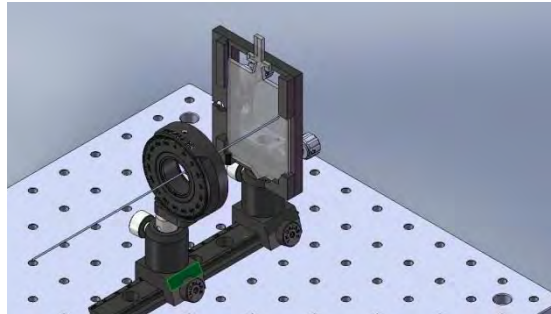


**Figure 83 - Fixturing system on an alignment rail.**

Further, we are construing concepts to migrate these conditions to the eventual illumination system required to achieve patterns upon the ultimate spherically shaped devices. One important element of the future system will be to incorporate a real time metrology system which will be capable of witnessing the virtual image plane of the master and allow us to dynamically position the substrates to achieve a substrate focused image, much in the same method as in a semiconductor wafer leveling process. Other considerations for this system will depend largely upon the desired pattern, feature size and across field uniformity of the patterned area. Initial discussions on this topic suggest that we translate the existing condition of exposure to curved substrates to explore the process window and realized efficiency of such a device as we define the requirements for a three dimensional exposure system.

### 2.3.3 Curing System

A curing system was developed to crosslink the LCs after deposition, Figure 84. The system consisted of a UV-crosslinking oven (UVP CL-1000 crosslinking oven) which delivers  $0.4 \text{ mW}$

of power at 365 nm. A consistent nitrogen flow was fed into the oven through a needle valve, and regulator pressure was set at 5 psi. The oven chamber was purged with nitrogen for 60 s before introducing plaques to cure, which allowed the UV lamps to warm up. Temperature inside the UV oven could reach 35 °C if left on continuously. Curing time for plaques selected for the current study was 300 s.

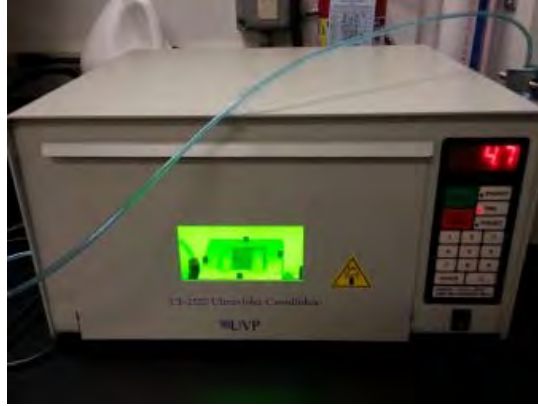


Figure 84 - Curing Oven

#### 2.3.4 Plaque Tooling and Production

During the thin film process development phase we determined that some inconsistency in the flatness of the plaques molded from our current tooling was contributing to inconsistent coating results. To resolve the issue we had two inserts made to fit into the Revision master unit die Frame with additional ejector pins to ensure the parts are being ejected without distorting the part. This was also done to enable full automation of the molding process for a more consistent cycle and improvement in surface quality for coating of thin films. 2000 plaques were made for the UCHET program in roughly one eight hour shift, saving hundreds of hours of molding plaques with the mini injection molder, and greatly reducing inconsistency between parts.

#### 2.3.5 Imaging Metrology

Imaging methods were utilized to create a surface model using the Beer-Lambert relationship:

By taking images of a coated substrate,  $A(x, y)$  and a blank substrate for calculating a flat field  $FF(x, y)$ , a surface plot may be constructed, using an estimate for the extinction coefficient,  $\alpha=0.0014/\text{nm}$ .

$$T = \frac{I}{I_0} = 10^{-\alpha l} \Rightarrow l = -\log\left(\frac{I}{I_0}\right)/\alpha$$

Where  $T$  is the transmission,  $\alpha$  is the extinction co-efficient,  $I$  is the measured intensity at a particular pixel of the coated substrate,  $I_0$  is the measured intensity of the uncoated substrate at the same pixel, and  $l$  is the calculated thickness of the alignment layer at that point.



## Uniform Alignment Layer on Polycarbonate Coating Example

The images in Figure 85 and Figure 86 were taken of an early uniform alignment layer (Trial B03) and a blank substrate using identical exposures and were registered using commercial image processing software (Photoshop). They were converted to grey-scale, processed with Beer's law in MATLAB, and then further analyzed with ImageJ for ease of manipulation. Each image is approximately 14 mm across. The white bar in the right-center region is a spectral error due to the microscope's optics, and can be seen in almost all the pictures included in this report.

Figure 87 is the 3D surface map of Figure 86 subtracted from Figure 85, which shows a mostly uniform coating with some surface defects. It can be seen that standard deviation of the surface, a good indication of roughness, can be seen as 7.8 nm, with a mean of 54.5 nm. The trough is an artifact due to the microscope optics and should be ignored. Figure 88 is the thickness distribution of the coating in nanometers.



Figure 85 – Uniform alignment layer



Figure 86 – Blank substrate

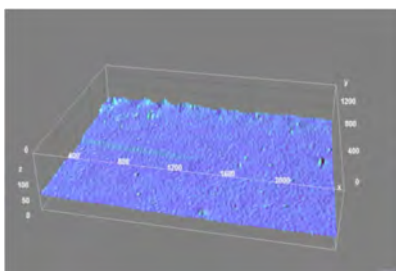


Figure 87 - Topographic Map

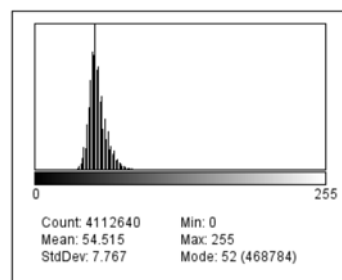


Figure 88 - Thickness distribution (nm)

## Imaging Metrology Summary

An imaging microscope with fixed, manual exposure parameters was utilized to image various coated and uncoated substrates. While this method provides an adequate precision for current studies, reduction in uncertainties in the extinction co-efficient, and additional camera linearity tests need to be done to further increase both the precision and accuracy of these methods. These methods also lend themselves to semi-automated defect measurement, though these defect rates have only recently moved into a realm where meaningful statistics may be collected.

### 2.3.6 Root Cause Analysis of Dewetting at AZB and LC Layer Interface

As progress was made in the spray coating of the AZB we first validated the capability by spin coating the LC layer upon the coated AZB plaques. The results were acceptable; however, it became evident that extreme care would be required to achieve defect free coatings due to either

substrate imperfections, and/or foreign material contamination as witnessed by premature crystal germination within the layer. These concerns can be easily addressed with proper substrate manufacturing and polishing, and by conducting the process in a sufficiently clean environment.

Spray coating of the LC layer: As in the case of the AZB spray coating, it was quickly found that some form of surface treatment would be required to promote proper adhesion and uniform film thickness.

The conditions observed during spray coating instantly resembled an issue of de-wetting, or a phobic surface condition to the LC material rather than a desired philic condition. To verify compatibility with the USI spray coat system a battery of experiments, substrates and systems were explored to determine the feasibility of obtaining the required thin film of LC over AZB.

Initial tests included blank and hard coated substrates. The surface treatment required was similar to that of the primary AZB layer, suggesting a specific trait of the LC polymer exhibits a similar chemical makeup resembling a polarized molecule characteristic and would need to be matched to the AZB surface to achieve the proper film. After a handful of baseline steps, we were able to determine that the LC layer could be spray coated with acceptable quality upon bare substrates much under the same conditions that AZB is spray coated. This situation is illustrated in Figure 89.

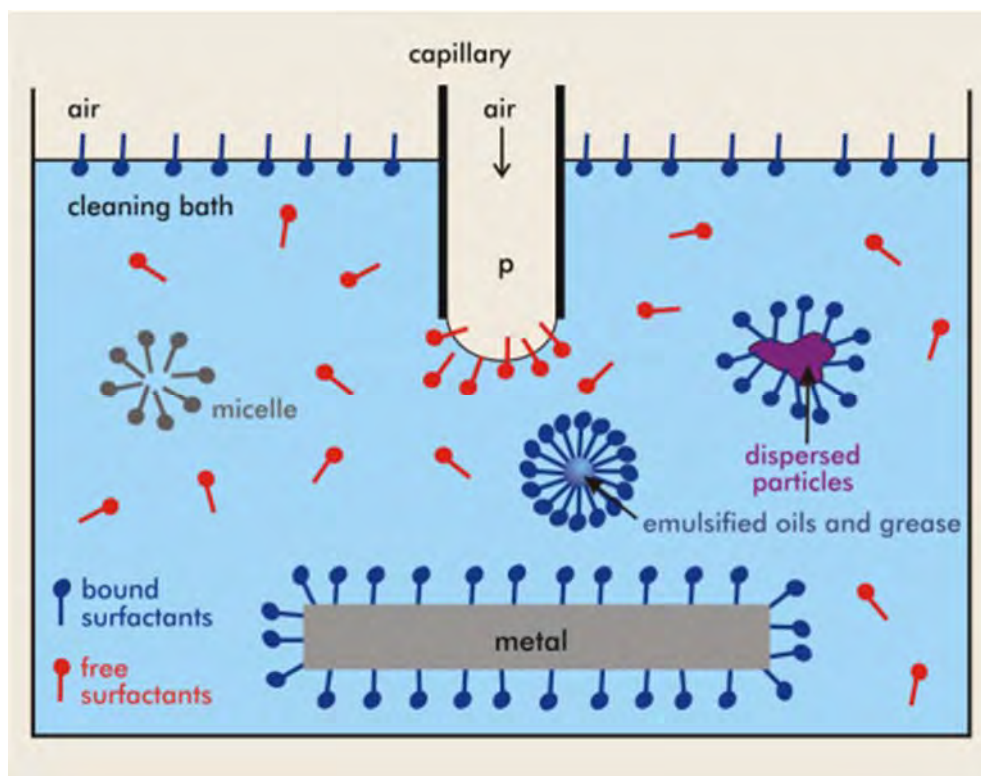


**Figure 89 - Highly polarized surfactant molecules demonstrating hydrophobic and hydrophilic conditions** (J. Ruchmann, 2008)

Evaluating a generic AZB molecule, as in Figure 90, one can see that the molecule requires some form of modification for optimizing the material with subsequent process layers. This is

typically done with modified surfactants to promote attraction with the substrate and further process layers. Also, it is pointed out that the AZB used in this program has been most likely optimized for other types of deposition processes, as was the LC layer. AZB itself can be formulated for a variety of functions and conditional responses within the bulk material as well as with the exposure sensitivity and process latitude.

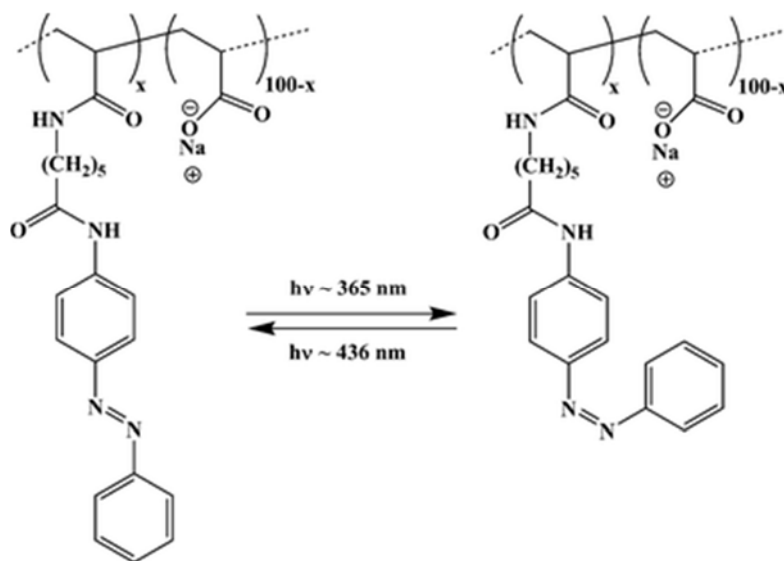


Figure 90 - Cis-trans conformation change(J. Ruchmann, 2008)

For this application, we are assuming that it has been matched on one or more of these characteristics for application with the LC polymer. It is also our understanding that the LC layer is the critical material in the program, meaning that we would be more likely to modify the AZB layer to be compatible with the LC layer, than vice versa.

Evaluation of the basic LC reaction to the AZB strongly resembles an interaction similar to that of a fluorinated compound, much like a Teflon treatment as commonly observed with automotive windshields coated with “Rain-X”, a Teflon based material. The highly phobic surface of the AZB to the LC causes the LC layer to bead up instantly when spray coated.

Options to Improve LC coating:

(1) Surface treatment:

Surface treatment is greatly limited by requirements of preserving the surface layer and interface required to properly achieve LC alignment to the patterned AZB. This eliminates many options with respect to additive process materials, as we need to preserve the relationship (direct contact) to the LC layer. Some other surface treatment processes may also be considered, such as remote plasma exposure to either increase or decrease the polarity of the surface top layer by grating appropriate chemical groups.

Subtractive processes being the alternative, and being successful in the corona treatment of the base substrates, we explored similar cleaning, de-scum, and plasma treatments to reveal a surface which might promote wetting of the LC material. Little no change was observed.

## (2) Tool parameters:

Suspecting that the spin coat process was successful, we evaluated parameters within the spray coat system, which might emulate the kinetic forces occurring during spin coat. These parameters include atomizing nozzle power, physical proximity, flow rates, drive air, and stage speeds.

To accelerate the evaluation process, we brought materials to USI where we enlisted the support of an applications engineer and a technician to rapidly complete a matrix of experiments to find the optimal parameters. Within a few tests, we determined an improved set of spray conditions, and were able to achieve high quality coatings with witness test substrates, thereby proving the USI system's ability to spray the LC material. With these conditions in hand, we transitioned to the AZB coated blanks and achieved good initial quality coatings, but before the substrate could be removed from the system, (seconds) the LC layer began retracting towards the center of the substrate. Further manipulation of the machine conditions yielded no better result than the first coatings, and pointed towards a definite materials interface incompatibility.

## (3) Process parameters:

Understanding that steps 1 and 2 above had limitations and narrow equipment operating parameters we shifted focus to modifying the process conditions of the spray coating process. This included changing the concentration of the material % solids, carrier solvent, and temperature of the spray coating.

While some improvements were noted by changing the solvent, a repeatable improvement was realized when the substrate was heated to a temperature of 50 °C. However, only a single pass with a limited width of ~1 cm, (limited by current nozzle) was achieved. Any serpentine spray patterns caused degradation to surrounding coatings. This suggests that the carrier solvent of the LC behave similarly to a traditional photo-lithography resist material, such as an acrylate based solution, and requires a slightly elevated temperature during coating. The elevated temperature of the substrate allows the LC material to land upon the substrate, but then dry quickly before the material is allowed to pull back, as in the "moist" conditions observed at USI. Subsequent passes did not have the benefit of pristine surface conditions, as overspray was present across the remainder of the substrate, and therefore was not able to achieve the initial wet like conditions needed for finish quality.

One possible solution to the coating may be to design a custom nozzle capable of coating the entire substrate area in a single pass.

## (4) Chemical modification

Ultimately, modifying the chemistry of either of the layers is required for an ideal solution. The additives and cleaning processes explored in our efforts were not enough to overcome the materials interactions between the AZB and the LC. We believe that the best solution will be to modify or change the chemistry of the AZB and LC solvent systems, so that they behave better in the spray coater.

### 3.0 RESULTS AND DISCUSSION

The morphology of the functional coatings is of crucial importance for their physical properties and the structure of each layer in a multilayer optical device affects the device performance. The operation of those based on polymers depends especially strongly on film morphology. Therefore, precise control of the molecular orientation and morphology of organic coatings is critical in the manufacturing of thin film optical devices including those used as light filters, emitters or absorbers for Near UV, Visible and Near Infrared regions. The rapid and on-demand-activated optical device based on diffractive wave-plates requires depositing gratings of high efficiency in micron-thick material layers.

Typically, solution processed organic multilayer devices, such as solar cells or organic light emitting diodes, are cast from highly diluted solutions. Other techniques include knife coating, die coating or, for thinner uniform films, jet printing and spin coating. Within this project, spray-coating technique was investigated as an alternative method of depositing uniform, thin organic films especially useful for curved plastic substrates such as eyewear lenses and visors.

Ultrasonic spray coating can be used for delivering a precisely controlled amount of film forming material onto the curved substrate, including cylindrical, spherical or more complex geometries. In some aspects, including atomization process, dynamics of mechanical deformation/coalescence of droplets and their size distribution, this type of thin film deposition is unique. However, in other aspects such as kinetics of drying, time dependence of solid content, surface tension and viscosity, gelation point, possible vertical/lateral phase separations, and dependence on rheological behavior of a liquid, spray coating is similar to other techniques of organic film deposition. Its result strongly depends on chemical and physical interactions at the coating/substrate interface, solvent evaporation, local temperature, initial solids content, miscibility of components, etc.

Spray coating of thin AZB layers (of average thickness  $<100$  nm) occurred at so-called dry coating mode, where the mechanical splashing of droplets caused formation of deformed circular rings determining surface profile. It was due to rapid evaporation of the majority of the solvent, the hysteresis of contact angle and possibly due to transport of the material towards the drying edge of the droplet. The latter mechanism was observed for larger droplets of the same material during microscopic examination. More droplet coalescence was observed for AZB coating, which suggested that the liquid might contain slower evaporating solvent. Figure 91-93 show the AZB coating compared to a reference dye coating, both observed in reflected light. The vertical lines in Figure 91 are due to imperfections in the substrate surface.



**Figure 91 - Surface profile of the AZB coating on hard-coated PC plaque.**

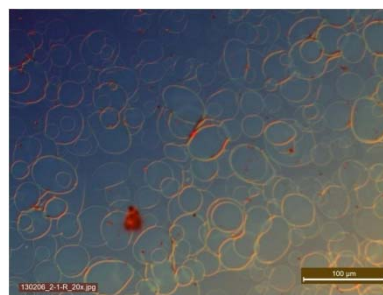


**Figure 92 - Reference dye coating, reflected light**

The surface profiles described above were observed for hard-coated PC plaques with surfaces modified by exposure to corona treatment, which increased compatibility between substrate and the drying liquid. For AZB coatings thicker than 100 nm deposited on untreated hard-coated PC, complete dewetting was observed, where the entire liquid formed a collection of droplets of various sizes – not compatible with size distribution created by the spray coater. Larger droplets showed the inner structure, suggesting partial crystallization of its component(s). Figure 93 shows such a circular spot of AZB coating.

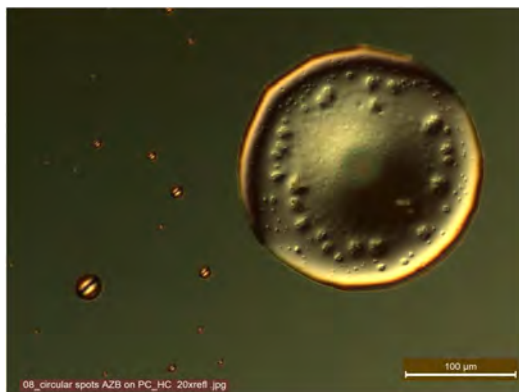


**Figure 93 - Partial crystallization**

In contrast to AZB, spray coating of LC layers (of average thickness  $\sim 1 \mu\text{m}$ ) occurred at so-called wet mode, where the amount of materials delivered to the substrate surface was high enough to cause rapid coalescence of droplets, leading to formation of a relatively thick liquid film. During drying, the characteristic film phenomena were observed. They included local or complete dewetting of the substrate (here, the previously deposited AZB layer) and crystallization of the material. The latter showed formation of several types of crystallites (described in 2.3.1.5 and 2.3.1.6) and likely a two-component kinetics of crystallization, namely a short-term component involving rapid formation of oriented structures during the last phases of film drying, and a long-term component involving crystallization during sample storage after UV curing.

Figure 94 and Figure 95 show the HC/AZB/LC coated PC samples before and after 1 and 2 months of storage in laboratory conditions. Long-term crystallization is most likely due to insufficient crosslinking of the produced gratings or due to presence on non-crosslinkable LC component of lower molecular weight. Figure 96 shows the typical crystallization that occurs with the LC after deposition, curing, and storage for roughly two months.

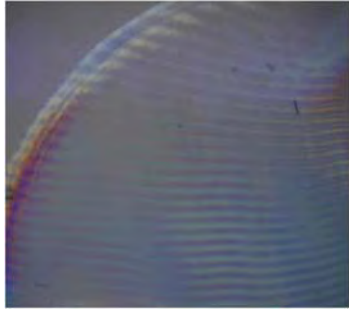


**Figure 94 - LC coated and patterned PC samples after 5 days, cross polarizers**

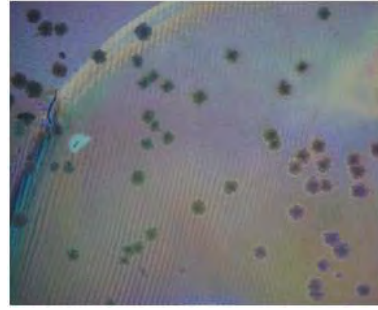


**Figure 95 - LC coated and patterned PC samples after 1 month storage, cross polarizers**

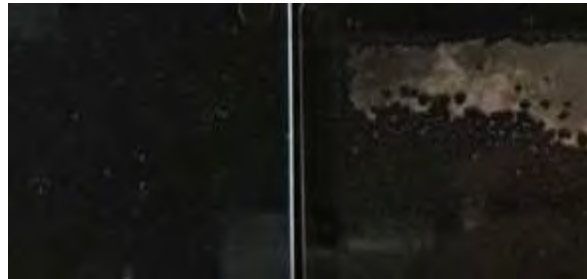


**Figure 96 - Comparison of samples just produced and the one stored for ~ 2 months, observed in reflected light on black background.**

Dewetting phenomena, described above in 2.3.1.5 and 2.3.1.6, were due to profound mismatch between surface free energy of the dried and UV exposed AZB layer and freshly deposited LC coating. We were able to prove that the dewetting takes place at the AZB/LC interface and that the AZB coating was not destroyed by drying LC liquid. As mentioned above, the obvious reason of observed dewetting was incompatibility of AZB surface polarity with polarity of LC coating liquid.



## 4.0 CONCLUSIONS

Both the AZB and LC materials can be spray coated onto the same polycarbonate material as used in Revision's military grade ballistics protective eyewear using the ultrasonic spray coater. The LC coating should be deposited on the lens preferably in a single pass of the ultrasonic head over the entire surface. This may require using a spray coater with wide or multiple ultrasonic heads. However, we found that the process window where we were able to obtain an acceptable thin film in a single pass is small.

Basic compatibility of AZB and LC materials with the ultrasonic spray coating method was verified at USI (Application Laboratory in Massachusetts) by spraying LC solution onto polyethylene terephthalate and bare polycarbonate. In both cases, the films wet the surface properly, suggesting that modifying the substrate surface (AZB layer) should improve wettability.

As a reference, uniform coatings of AZB and LC on glass and HCPC substrates were obtained by spin coating, which reproduces the work done elsewhere. It showed that dewetting can be overcome due to different kinetics of physical phenomena occurring in spin coating processes such as film spreading, solvent evaporation and material gelation.

The surface of AZB coating produced using existing liquid formulation is fundamentally chemically incompatible with the LC material in cyclopentanone. There is a strong tendency for LC dewetting when a thin LC film is formed using a spray coating method on the thin film of previously deposited AZB, both with and without exposure to alignment irradiation procedure. Ultrasonic spray coating atomizes the LC mixture into many droplets with relatively narrow size distribution, which splashes on the substrate surface and coalesces. Our understanding is that slower drying, absence of centripetal forces and longer time scale of ultrasonic spray coating allow surface tension forces to act before the gelation point of the LC material is reached during drying. This allows revealing incompatibility of AZB surface with the LC solution observed as a mismatch of molecular interactions at the interface. Depending on spray coating parameters, this may cause local or complete dewetting.

We found that the surface of HCPC substrate can be treated by corona discharge in air before depositing the AZB coating. This improves wettability in the system and allows for formation of a uniform alignment film of required thickness.

In the LC coatings deposited on the AZB layer and on HCPC directly using an ultrasonic spray coater, we observed crystallization that depended on thickness of the LC coating. Thicker layers, including those in the required thickness range ( $\sim 1.5 \mu\text{m}$ ), had a higher tendency to crystallize, while thinner layers were prone to produce local dewetting. Crystallization defects emerge in two-component kinetics, namely in short and long time scale. First, the crystallization occurring during the first few minutes is observed in uncured LC coatings, and the second during a few months of storage at laboratory conditions after UV curing.

It seems that longer or stronger LC curing may be required to avoid long-term crystallization. Alternatively, the amount or character of the UV curing initiator may be changed in the LC solution.



#### **4.1 Implications for Future Work**

It is important to develop material formulations that can produce an improved LC/cyclopentanone compatible coating. The new formulation should lead to the surface on which the LC solution would show very low static contact angle and spread easily wetting the entire surface. We believe that modifying AZB solution should be easier than changing components of LC; however, this opinion is open for discussion.

Alternatively, it may be advisable to develop a surface treatment of AZB layer applied before or after laser irradiation and before coating with LC. The treatment may involve surface grafting of selected chemical groups by dry methods such as a combination of remote plasma and exposure to reactive vapors.

From the perspective of the device development, it is important to use exactly the same AZB and LC formulations during the entire project, including active components, solvents, and their concentrations. After the LC-compatible AZB is formulated, its composition should remain the same.

## 5.0 REFERENCES

J. Ruchmann, S. F. (2008). Light-responsive hydrophobic association of surfactants with azobenzene-modified polymers. *Soft Matter* , 2098-2108.

Siew-Lay Lim, E.-C. C.-Y.-H.-K.-F. (2012). High performance organic photovoltaic cells with blade-coated active layers. *Solar Energy, Materials, & Solar Cells* , 292-297.

## List of Symbols, Abbreviations, and Acronyms

AZB	- Azobenzene
HC	- Hard Coat
HCPC	- Hardcoated Polycarbonate
LC	- Liquid Crystal
MEK	- Methyl Ethyl Ketone
UCHET	- Ultrasonic Coating and Holographic Exposure Technology
USI	- Ultrasonic Systems, Incorporated
UV	- Ultra Violet